Triheteromeric NR1/NR2A/NR2B receptors constitute the major NMDA receptor population in adult hippocampal synapses

INAUGURAL-DISSERTATION

zur
Erlangung der Doktorwürde
der
Naturwissenschaftlich-Mathematischen Gesamtfakultät
der
Ruprecht-Karls-Universität
Heidelberg

vorgelegt von
Diplom-Pharmazeutin Claudia Rauner
aus Mannheim

INAUGURAL-DISSERTATION

zur
Erlangung der Doktorwürde
der
Naturwissenschaftlich-Mathematischen Gesamtfakultät
der
Ruprecht-Karls-Universität
Heidelberg

vorgelegt von
Diplom-Pharmazeutin Claudia Rauner
aus Mannheim

Tag der mündlichen Prüfung:

Triheteromeric NR1/NR2A/NR2B receptors constitute the major NMDA receptor population in adult hippocampal synapses

Gutachter: Priv.-Doz. Dr. Georg Köhr
Prof. Dr. Gert Fricker

Erklärung gemäß §8 (3) b) und c) der Promotionsordnung:
Hiermit erkläre ich, dass ich die vorliegende Dissertation selbst verfasst und mich dabei keiner anderen als der von mir ausdrücklich bezeichneten Quellen und Hilfen bedient habe. Des Weiteren erkläre ich, dass ich an keiner anderen Stelle ein Prüfungsverfahren beantragt oder die Dissertation in dieser oder einer anderen Form bereits anderweitig als Prüfungsarbeit verwendet oder einer anderen Fakultät als Dissertation vorgelegt habe.

Heidelberg, 23. 02. 2010 _____

Dedicated to Harald, my and his family

Zusammenfassung

N-Methyl-D-Aspartat-Rezeptoren (NMDARen), die eine wichtige Rolle bei Lern- und Gedächtnisprozessen spielen, aber auch für bestimmte neurologische Störungen verantwortlich sind, sind heterotetramere Komplexe, die aus zwei NR1- und zwei NR2-Untereinheiten bestehen. Die Rolle synaptischer NMDARen in postnatalen Prinzipalneuronen im Vorderhirn wird entgegen zwingenden Beweisen für triheteromere NR1/NR2A/NR2B-Rezeptoren in der Regel diheteromeren NR1/NR2A- und NR1/NR2B-Rezeptoren zugeschrieben. In hippokampalen CA1-Synapsen konnten die Eigenschaften triheteromerer Rezeptoren bislang nicht von denjenigen diheteromerer NMDAR-Mischungen unterschieden werden. Um NR1/NR2A/NR2B-Rezeptoren charakteristische Eigenschaften zuzuweisen, wurden in der vorliegenden Arbeit zwei verschiedene, jeweils ausschließlich reine NR1/NR2A- oder NR1/NR2B-Rezeptorpopulationen exprimierende, *NR2 knockout*-Mauslinien eingesetzt und deren synaptische Eigenschaften mit denen der Wildtyp-Mäuse verglichen. Es stellte sich heraus, dass die beiden diheteromeren NMDAR-Subtypen in akuten hippokampalen Schnitten adulter Mäuse eine unterschiedliche Spannungsabhängigkeit der Deaktivierungskinetik aufwiesen. Bei Wildtyp-Mäusen vergleichbaren Alters konnten wir nur die NR1/NR2A-charakteristische Spannungsabhängigkeit der Deaktivierungskinetik beobachten. Dies bedeutet, dass NR1/NR2B-Rezeptoren nur eine kleine Population in adulten CA3-CA1-Synapsen ausmachen. Stattdessen trat das Vorhandensein von NR1/NR2A/NR2B-Rezeptoren aufgrund einer langsameren Deaktivierungskinetik der NMDA-Ströme (NMDA EPSCs) als derjenigen der reinen NR1/NR2A-Rezeptoren deutlich hervor. Darüber hinaus untersuchten wir den Effekt von NR2B-Untereinheit-bindenden NMDAR-Antagonisten auf NMDA EPSCs in der Abwesenheit von extrazellulärem Mg^{2+}, was die Sensitivität der Antagonisten, insbesondere für NR1/NR2A/NR2B-Rezeptoren, stark verbesserte. Der Effekt dieser Antagonisten auf NMDA EPSCs war stark bei P5 und blieb bei circa 50 % bei P28. Folglich ist die NR2B-Untereinheit in hippokampalen Synapsen während der gesamten Entwicklung von Bedeutung und wird in adulten Mäusen in Form von NR1/NR2A/NR2B-Rezeptoren bewahrt.

Summary

N-methyl-D-aspartate receptors (NMDARs), fundamental to learning and memory and implicated in certain neurological disorders, are heterotetrameric complexes composed of two NR1 and two NR2 subunits. The role of synaptic NMDARs in postnatal principal forebrain neurons is typically attributed to diheteromeric NR1/NR2A and NR1/NR2B receptors, despite compelling evidence for triheteromeric NR1/NR2A/NR2B receptors. In hippocampal CA1 synapses, the properties of triheteromeric NMDARs could thus far not be distinguished from those of mixtures of diheteromeric NMDARs. To find a signature of NR1/NR2A/NR2B receptors, we have employed two gene-targeted mouse lines, expressing either NR1/NR2A or NR1/NR2B receptors without any NR1/NR2A/NR2B receptors, and compared their synaptic properties to those of wild type. We found in acute hippocampal slices of adult mice a distinct voltage dependence of NMDA EPSC decay time for the two diheteromeric NMDARs. In age-matched wild-type mice, only the NR1/NR2A characteristic for this voltage-dependent deactivation could be detected, indicating that NR1/NR2B receptors are a minor population in adult CA3-to-CA1 synapses. Instead, the presence of NR1/NR2A/NR2B receptors became manifest from a slower NMDA EPSC decay time than for NR1/NR2A receptors. Moreover, we examined the sensitivity of NMDA EPSCs to NR2B-directed NMDAR antagonists in the absence of extracellular Mg^{2+}, which improved the sensitivity of these antagonists, especially for NR1/NR2A/NR2B receptors. NMDA EPSC sensitivity to NR2B-directed NMDAR antagonists was high at P5 and remained around 50% at P28. Thus, NR2B is prominent in hippocampal synapses throughout life and remains present in adult mice as an integral part of NR1/NR2A/NR2B receptors.

Contents

1 Introduction

1.1 Signal transmission in the central nervous system

The nervous system is an organ system consisting of a network of nerve cells (neurons) and glial cells. It receives incoming information about the organism and the environment, which is further processed in order to trigger an appropriate action. In most animals, the nervous system consists of two parts, central and peripheral. The central nervous system (CNS) integrates incoming stimuli, originating either from the organism itself or from the environment, it coordinates all motor action and regulates the communication between different organs and systems. In humans and all other vertebrates, the CNS comprises the brain and the spinal cord. The human brain consists of 10^{11} neurons and 10 times more glia. In the classical view, glial cells have been considered to play simple supportive roles for neurons. They were thought to provide the brain with structure, sometimes insulate neuronal groups and synaptic connections from each other. Certain classes of glial cells guide migrating neurons and direct axonal outgrowth. Furthermore, they help to form the blood-brain-barrier, remove cellular debris and secrete trophic factors. However, this view of glia representing only passive bystanders of the neural transmission has changed, since recent research indicates that glial cells participate in synaptic transmission, are able to modulate synaptic strength, and even release neurotransmitters (Haydon and Carmignoto, 2006; Henneberger et al., 2010; Perea and Araque, 2009). But, although the dogma that synaptic function results exclusively from signaling between neurons as the only excitable cells has been challenged by the finding that glial cells can also fire action potentials (Káradóttir et al., 2008), the signaling by neurons is still indispensable.

Neurons are classically divided into two functional classes: principal (or projection) neurons and interneurons. Principal neurons, possessing long-distance projections, convey information from organs and tissues to the CNS (afferent neu-

rons), or transmit signals from the CNS to the effector cells (efferent neurons) that can be located in other networks within the CNS or in tissues outside the CNS, like e.g. muscles. Principal neurons can be either excitatory with glutamate as the most important excitatory neurotransmitter, or inhibitory. In contrast to principal neurons, interneurons are only locally projecting and connect neurons involved in the same processing state within specific regions of the CNS. Interneurons are often inhibitory and use the neurotransmitters GABA or glycine. Inhibitory neurons control spike timing of principal neurons, synaptic plasticity, and network oscillations (Bonifazi et al., 2009; Buzsáki and Chrobak, 1995; Paulsen and Moser, 1998; Whittington and Traub, 2003).

Although neurons are very diverse and show different sizes and morphologies depending on their function and location, a schematic description of the structure and function of a 'typical' neuron can be given (Fig. 1). A typical neuron is divided into three parts: soma or cell body, dendrites, and axon. The soma contains the nucleus and other organelles important for protein synthesis and homeostasis. Multiple dendrites extrude from the soma and branch multiple times, giving rise to the dendritic tree. Neurons receive input from other neurons over the dendrites, which often exhibit small protrusions, called spines. Signals to other neurons are transmitted by the axon, the output structure of the neuron. It arises from a swelling of the soma, the axon hillock, and also shows extensive branching. The structures contacting other neurons are typically the presynaptic terminals or boutons, which appear as a thickening at the end of the axon. The contact between the axonal bouton of one neuron, called presynaptic neuron, and the dendritic spine or another part of the other, postsynaptic neuron, is called 'synapse'.

Neuronal communication or synaptic transmission can take place either electrically or chemically. Electrical signaling is fast and without latency, because at electrical synapses signals are transmitted by direct exchange of ions via gap junctions which form a contact between the pre- and the postsynaptic neuron. In contrast, at chemical synapses, the pre- and postsynaptic neurons are separated by the synaptic cleft and therefore electrically isolated. Here, signal transmission requires neurotransmitter release and diffusion, making chemical signaling slower compared to electrical signaling.

The special feature of neurons, enabling them to the reception and transmission

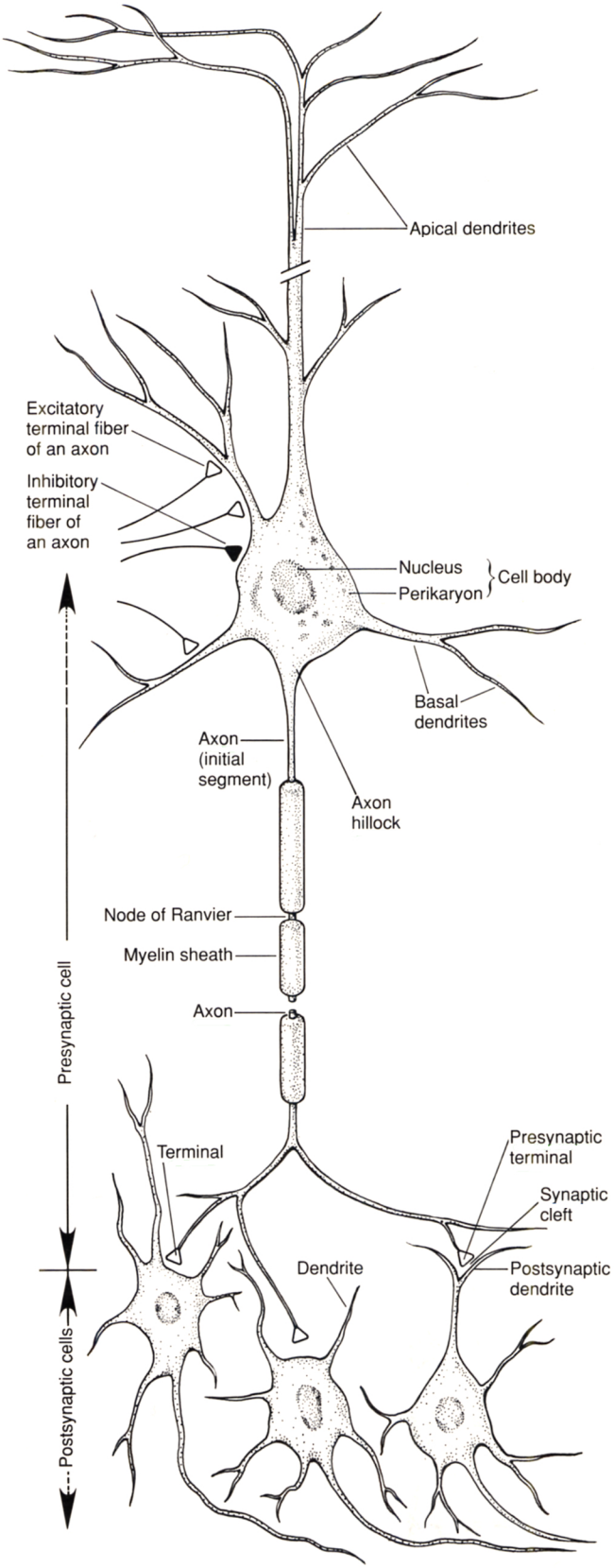

Fig. 1: Morphology of neurons. The cell body contains nucleus and perikaryon, and gives rise to two types of processes: dendrites and axon. Axons, the transmitting elements of neurons, can vary greatly in length. The axon hillock is the site at which the action potential is initiated. Many axons are insulated by a myelin sheath that is interrupted at regular intervals by regions known as nodes of Ranvier. Branches of the axon of one neuron (the presynaptic neuron) transmit signals to another neuron (the postsynaptic neuron) at a site called synapse. The branches of a single axon may form synapses with as many as 1000 other neurons (adapted from Kandel et al., 2000).

of signals, is their electrical excitability. A combination of special ion channels and metabolically driven ion pumps maintains a voltage-gradient across the semipermeable membrane by intracellular-versus-extracellular concentration differences of ions such as Na^+, K^+, Ca^{2+}, and Cl^-. The resting membrane potential ranges typically from -80 mV to -60 mV, depending on the cell type. If the membrane is depolarized by excitatory inputs and reaches a certain membrane potential threshold (typically -40 mV), an action potential, which is an all-or-none event and has a stereotyped shape, is generated. The ability of neurons to generate an action potential, a regenerative electrical output signal, is the basis of signal transmission in the CNS. The action potential is initiated in the axon hillock and then spreads along the axon without attenuation. Additionally, it propagates back into the dendrites and therefore provides a retrograde signal of neuronal output to the dendritic tree. Reason for the generation and specific properties of the action potential is the presence of diverse ion channels in the plasma membrane, mainly of voltage-activated Na^+ and K^+ channels. As soon as excitatory stimuli depolarize the negative resting membrane potential above a certain threshold, voltage-activated Na^+ channels have a higher open probability. The opening of these voltage-activated Na^+ channels results in further depolarization by an influx of Na^+ ions, and the membrane potential is driven towards the equilibrium potential for Na^+ (around $+50$ mV). Before the maximum membrane potential is reached, the voltage-activated Na^+ channels rapidly inactivate. Voltage-activated K^+ channels have a similar threshold as voltage-activated Na^+ channels, but their opening is much slower, so that they reach their maximum when most of the voltage-activated Na^+ channels are already inactivated. This leads to an K^+ outflow and repolarizes the cell membrane. Action potential propagation along the axon can either be continuous, as for non-myelinated axons, or saltatory, as for myelinated axons. In non-myelinated axons, an action potential depolarizes the surrounding membrane, so that the threshold is reached and a new action potential is generated in the vicinity of the primary action potential. This spread of excitation is relatively slow (most of the times only 1-3 m/s, at maximum 30 m/s). In vertebrates, most of the axons are myelinated. The myelin sheath is formed by glial cells and is interrupted at regular intervals by regions called nodes of Ranvier. The isolation by the myelin sheath markedly accelerates the speed of conduction.

The positive charges spread along the axon, and the amplitude of the initial action potential is regenerated at the nodes of Ranvier, which constitute the only places where action potentials can be generated along the myelinated axon.

When an action potential arrives at the presynaptic terminal, voltage-sensitive Ca^{2+} channels open. The subsequent Ca^{2+} influx binds to proteins that trigger the fusion of neurotransmitter-filled presynaptic vesicles with the plasma membrane. The neurotransmitter is released into the synaptic cleft and diffuses across the synaptic cleft to the postsynaptic membrane. There, it binds to postsynaptic receptors leading to opening or closing of ion channels, and thereby altering the membrane conductance and potential of the postsynaptic cell.

Receptors can be of two different types, ionotropic or metabotropic. Ionotropic receptors are transmembrane ion channels that open or close in response to the binding of a neurotransmitter and mediate fast synaptic transmission in the millisecond range. In contrast, metabotropic receptors do not form an ion channel, but are indirectly linked with ion channels through signal transduction mechanisms, using G-proteins as second messengers. Therefore, they act on a slower time scale in a second-to-minute range.

Synaptic transmission in the CNS can be either excitatory or inhibitory, depending on the released neurotransmitter and the activated receptors. Glutamate is the predominant chemical transmitter of excitatory synapses (Curtis et al., 1959), and receptors for this ubiquitous neurotransmitter are divided into two classes: ionotropic and metabotropic. Ionotropic glutamate receptors (iGluRs) are classified as L-α-amino-3-hydroxy-5-methyl-4-isoxazolepropionic acid (AMPA), kainate and N-methyl-D-aspartate (NMDA) receptors, based on their responsiveness to certain glutamate derivatives. All three types mediate a depolarizing current causing an excitatory postsynaptic potential (EPSP), but the speed and duration of the excitatory postsynaptic current (EPSC) is different for each type. The ionotropic glutamate receptors will be described in detail in the following section. In contrast to ionotropic glutamate receptors that always mediate an excitatory effect, metabotropic glutamate receptors can produce either excitation or inhibition, depending on the coupled G-protein.

The main inhibitory neurotransmitters in the CNS are glycine and γ-aminobutyric acid (GABA). GABA receptors are divided into ionotropic $GABA_A$ receptors and

metabotropic $GABA_B$ receptors. $GABA_A$ receptors form Cl^- and $HCO_3{}^-$ permeable channels which open upon GABA binding. The resulting anion influx, consisting mainly of Cl^-, mediates an inhibitory postsynaptic potential (IPSP) and rapidly hyperpolarizes the membrane. $GABA_B$ receptors can either activate K^+ channels or inhibit voltage-dependent Ca^{2+} channels.

The depolarizing and hyperpolarizing signals generated on the postsynaptic membrane at different excitatory and inhibitory connections spread along the dendritic tree. EPSPs and IPSPs are integrated and are either sub- or suprathreshold for the generation of an action potential.

1.2 Ionotropic glutamate receptors

1.2.1 Classification of ionotropic glutamate receptors

Most of the excitatory neurotransmission in the CNS is mediated by iGluRs. All iGluRs are ligand-gated, nonselective cation channels that are permeable for Na^+, K^+, and sometimes Ca^{2+} upon glutamate binding. Activation of iGluRs always leads to an EPSP, but the speed and duration of the underlying current (EPSC) is different for AMPA, kainate, and NMDA receptors, respectively. AMPA and kainate receptors, collectively termed as non-NMDARs, are responsible for a fast ionic inward current thereby contributing to the early peak of the EPSC. In contrast, NMDARs activate and deactivate relatively slowly compared to non-NMDARs and contribute mainly to the late phase of the EPSC (Mayer and Westbrook, 1987b). AMPARs form heteromeric complexes of the subunits GluR-A to GluR-D (GluA-1 to GluA-4), kainate receptors are subdivided into GluR-5 to GluR-7, KA-1, and KA-2 (GluK-1 to GluK-5) (Hollmann and Heinemann, 1994). The NMDAR subunits will be described in detail in the following sections. One additional family of the iGluRs, termed delta, was identified, but a functional profile has not been determined yet (Yamazaki et al., 1992). The two members of this class, $\delta 1$ and $\delta 2$, share 18 to 25 % sequence homology with the other iGluR subunits, but remain orphan subunits (Araki et al., 1993; Lomeli et al., 1993). Nevertheless, they seem to play important roles in the CNS, in particular in the cerebellum (Yuzaki, 2004; Zuo et al., 1997).

1.2.2 Structure of ionotropic glutamate receptors

iGluRs presumably assemble as tetramers in a dimer-of-dimers structure (Kim et al., 2010; Laube et al., 1998; Rosenmund et al., 1998; Sobolevsky et al., 2009): NMDARs are obligate heteromers (Monyer et al., 1992), whereas AMPA and kainate receptors can form functional homomeric complexes (Boulter et al., 1990), although in native tissues they have been shown to form almost exclusively heterotetramers (Christensen et al., 2004; Lu et al., 2009; Mulle et al., 2000). The specific subunit composition determines not only the biophysical properties of the GluR channel, but also its trafficking during basal synaptic transmission and synaptic plasticity (Barria and Malinow, 2002; Barry and Ziff, 2002). Although iGluRs are divergent with respect to function, electrophysiological profile, ion permeability, expression pattern, and trafficking, they are related in amino acid sequence and have a common structural design (Fig. 2). Each subunit comprises four modules (Wo and Oswald, 1995): the extracellular amino-terminal domain (NTD) participates in subtype-specific receptor assembly, trafficking, and modulation (Ayalon and Stern-Bach, 2001); the adjacent ligand-binding domain (LBD) is central to agonist binding and to activation gating (Stern-Bach et al., 1994). A transmembrane domain forms the ion channel (Wollmuth and Sobolevsky, 2004), and a cytoplasmic carboxy-terminal domain (CTD) influences receptor function, signaling, and trafficking (Barry and Ziff, 2002; Soderling and Derkach, 2000; Sprengel and Single, 1999). Each individual subunit consists of three transmembrane domains (M1, M3, M4) plus a cytoplasm-facing re-entrant loop (M2). The ligand-binding site consists of two globular domains (S1 and S2), that are formed by the sequence preceding the M1 domain and the M3-M4 loop. The S1 and S2 domains form a clamshell-like structure that undergoes a conformational change upon ligand binding (Dingledine et al., 1999; Stern-Bach et al., 1994). Residues in the re-entrant second membrane loop control key permeation properties of the ion channel (Wollmuth and Sobolevsky, 2004). The M2 region is thought to be involved in lining the channel pore and contains the functionally crucial Q/R/N site at its tip. The amino acid residues located at the Q/R/N sites most probably face the ion permeation pathway to form part of the selectivity filter in GluR channels (Burnashev, 1996). The Q/R/N site of the M2 segment is occupied by a glutamine

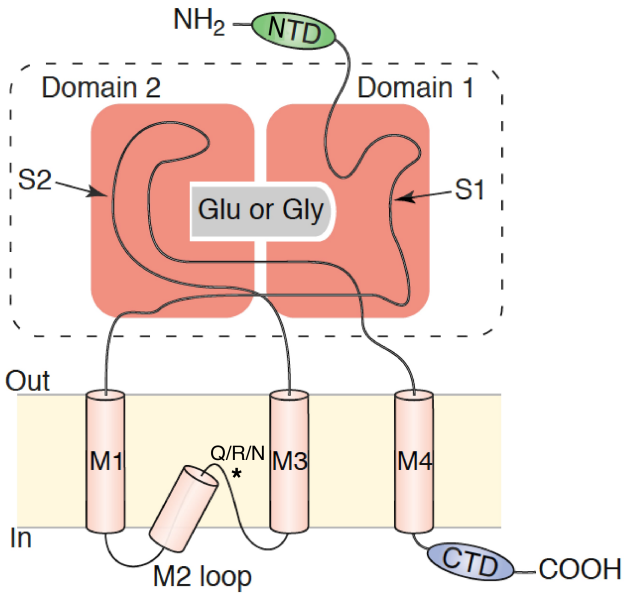

Fig. 2: Topology of ionotropic glutamate receptors. Individual glutamate receptor subunit with four hydrophobic segments, of which M1, M3, and M4 are membrane-spanning domains, whereas M2 forms a cytoplasm-facing re-entrant loop. The asterisk indicates the Q/R/N site. The S1 and S2 lobes form the ligand-binding domain (S1S2 complex, indicated by a broken line). The large extracellular NTD and intracellular CTD are not shown to scale (adapted and modified from Wollmuth and Sobolevsky, 2004).

(Q) or an arginine (R) residue in non-NMDARs and by an asparagine (N) residue in NMDARs. The Q/R/N site is also a site prone to RNA editing in AMPA and kainate receptors, with the GluR-B Q/R site being the most vigorously edited site (Higuchi et al., 1993; Sommer et al., 1991). Presence of edited or non-edited GluR-B in the heteromeric AMPAR channel determines the divalent ion permeability, e.g. Ca^{2+} (Burnashev et al., 1992a; Hume et al., 1991). Furthermore, the Q/R/N site affects single channel conductance and blockade by intracellular polyamines (Hume et al., 1991; Swanson et al., 1996). Thus, residues of the Q/R/N site constitute a common structural motif of the iGluR's M2 segment and influence some of their selectivity and conductance properties.

1.3 NMDA receptors

1.3.1 Role of NMDA receptors during synaptic transmission and plasticity

In neurons, NMDARs have been detected at both pre- and postsynaptic sites (Tzingounis and Nicoll, 2004). In GABAergic interneurons, NMDARs appear to be distributed along the smooth dendritic shafts, whereas in the postsynaptic membrane

of excitatory neurons, the density of NMDARs is higher in spines, within the postsynaptic density (PSD), than in the dendritic shaft and the somatic membrane. Among iGluRs, NMDARs have a unique function. For complete activation, they require simultaneous binding of an agonist and a coagonist, which can be either glycine or D-serine (Johnson and Ascher, 1987; Kleckner and Dingledine, 1988; Wolosker et al., 1999). The NMDAR pore is controlled in a voltage-dependent manner: at resting membrane potential, the receptor channel is blocked by Mg^{2+} and becomes unblocked due to depolarization (Nowak et al., 1984). The voltage-dependent Mg^{2+} block suites NMDARs to detect coincident presynaptic release of glutamate and postsynaptic depolarization. NMDARs are therefore coincidence detectors of pre- and postsynaptic activity. NMDARs are highly permeable to Ca^{2+}, so that under physiological conditions, Ca^{2+} constitutes $\sim$10% of the total NMDAR-mediated current (Burnashev et al., 1995; Jahr and Stevens, 1993; Mayer and Westbrook, 1987a; Schneggenburger et al., 1993). This Ca^{2+} influx can trigger intracellular signaling cascades leading to long-term potentiation (LTP) or long-term depression (LTD), which are thought to underlie memory acquisition and learning (Bliss and Collingridge, 1993; Dudek and Bear, 1992). Thus, the function of NMDARs is related to the induction of synaptic plasticity and to various forms of learning and memory. Furthermore, NMDARs are essential to the establishment and modification of synapses during development (Bear et al., 1990; Iwasato et al., 2000; Ramoa et al., 2001), but they are also involved into several pathophysiological processes (Cull-Candy et al., 2001; Meldrum, 1992; Rothman and Olney, 1995).

Activation of NMDARs can last for several hundred milliseconds (Hestrin et al., 1990; Lester et al., 1990). In comparison to non-NMDARs, which exhibit kinetics of activation[1], deactivation[2], and desensitization[3] on a millisecond timescale (Hansen et al., 2007), NMDARs show prolonged channel activity. The kinetic properties of NMDARs will be described in detail in section 1.3.5.

[1] opening of the receptor in the presence of agonist
[2] unbinding of agonist and closure of the channel
[3] closure of the channel with agonist bound

1.3.2 NMDA receptor subunits

To date, three gene families encoding for NMDARs have been identified: NR1, NR2 (A, B, C, D), and NR3 (A, B). NR1 and NR3A subunits have been described to undergo alternative splicing, which leads to further subclasses of several isoforms (Ciabarra et al., 1995; Moriyoshi et al., 1991; Nishi et al., 2001; Sasaki et al., 2002; Sucher et al., 1995; Sugihara et al., 1992; Sun et al., 1998). To form a functional NMDAR channel, two glycine/serine-binding NR1 and two glutamate-binding NR2 subunits presumably form heterotetrameric NR1/NR2 complexes composed of two diagonal heterodimers (Furukawa et al., 2005; Sobolevsky et al., 2009). In addition to these conventional NMDARs with known specific properties, NR1 and NR3 subunits can coassemble and form excitatory glycine receptors. By itself, glycine is usually thought of as an inhibitory neurotransmitter. However, NR1/NR3 receptors form excitatory glycine receptors that are insensitive to glutamate, Ca^{2+} impermeable, and resistant to Mg^{2+} (Chatterton et al., 2002). NR3A and NR3B differ with respect to their regional and developmental expression (Chatterton et al., 2002; Ciabarra et al., 1995; Fukaya et al., 2005; Sucher et al., 1995; Wong et al., 2002). Both NR3 subunits modulate NR1/NR2 heteromers by reducing current responses (Ciabarra et al., 1995; Das et al., 1998; Sasaki et al., 2002; Sucher et al., 1995), probably by assembling of NR1, NR2, and NR3 subunits into triheteromeric NR1/NR2/NR3 receptors (Cavara and Hollmann, 2008). It is still unclear whether the presence of NR3 results in a lower sensitivity to Mg^{2+} ions (Nishi et al., 2001; Sasaki et al., 2002; Sucher et al., 1995; Tong et al., 2008), though coexpression of NR3 appears to decrease the Ca^{2+} permeability of conventional NMDARs (Das et al., 1998; Matsuda et al., 2003, 2002; Pérez-Otaño et al., 2001). Thus, the NR3 subunit gives rise to a class of NMDARs with distinct properties from the conventional NMDARs. The key characteristics usually ascribed to NMDARs are determined by the conventional NMDARs, comprising two NR1 and two NR2 subunits. The NR2 subunits endow NMDARs with distinct biophysical and pharmacological properties, including deactivation, open probability, strength of Mg^{2+} block, single-channel conductance, and sensitivity to extracellular allosteric modulators (Cull-Candy and Leszkiewicz, 2004; Dingledine et al., 1999).

1.3.3 Developmental and spatial regulation of NMDA receptor subtype expression

The NR1 subunit shows continuous and ubiquitous expression in the brain, whereas expression of the four NR2 subunit genes, encoding NR2A-D, is temporally and spatially regulated (Monyer et al., 1994; Watanabe et al., 1993). NR2B and NR2D are present already during embryonic development, while expression of NR2A and NR2C starts after birth in the forebrain and the cerebellum, respectively. In hippocampal principal neurons, NR2D expression decreases postnatally and is no longer expressed in adulthood, in contrast to NR2B. Accordingly, immunogold labeling detected NR2A and NR2B in PSDs of adult CA1 pyramidal cells (Köhr et al., 2003). Hence, the predominant NR2 subunits in the adult hippocampus are NR2A and NR2B, giving rise to three different NMDAR subtypes: diheteromeric NR1/NR2A and NR1/NR2B receptors, as well as triheteromeric NR1/NR2A/NR2B receptors. Several studies suggested a higher content of NR2B-containing receptors at extrasynaptic than at synaptic sites (Fellin et al., 2004; Scimemi et al., 2004; Stocca and Vicini, 1998). In contrast, other studies have shown that NR2B remains present within the synapse (Fujisawa and Aoki, 2003; Janssen et al., 2005), and that NR2A-containing receptors are not only present within the synapse, but also extrasynaptically (Li et al., 1998; Thomas et al., 2006). This discrepancy indicates that the classification of NR2A as synaptic and NR2B as extrasynaptic NMDARs subunits is not absolute and that both subunits can be located either in synaptic or extrasynaptic compartments. Despite compelling evidence for NR1/NR2A/NR2B receptors (Al-Hallaq et al., 2007; Chazot et al., 1994; Kew et al., 1998; Luo et al., 1997; Sheng et al., 1994), the role of synaptic NMDARs in postnatal principal forebrain neurons is typically attributed to diheteromeric NR1/NR2A and NR1/NR2B receptors. The physiological roles of NR1/NR2A/NR2B receptors are difficult to address because, thus far, a signature of triheteromeric receptors allowing their distinction of mixtures of diheteromeric NMDARs is still not manifest.

1.3.4 Voltage-dependent Mg^{2+} block of NMDA receptors

The pore of the NMDAR channel is blocked by extracellular Mg^{2+} preventing ion influx (Mayer et al., 1984; Nowak et al., 1984). This voltage-dependent Mg^{2+} block is one of the unique properties that determines the critical contribution of NMDARs to CNS synaptic physiology. It imparts the receptor with the function of a coincidence detector, sensing simultaneous pre- and postsynaptic activity, which is a prerequisite for inducing input-specific, long-lasting changes in the strength of synaptic connections (Bliss and Collingridge, 1993).

In the pore-lining M2 segment of the NR1 and NR2 subunits, asparagine (N) residues occupy an identical position, called the N-site (Hollmann and Heinemann, 1994). In both subunits, these N-site asparagines are located at the tip of the loop formed by the M2 segment. The narrowest part of the pore, the narrow constriction or selectivity filter, is formed primarily by the N-site of the NR1 subunit and the N+1 site of the NR2 subunit, designating an asparagine residue adjacent to the N-site (Wollmuth et al., 1996). The narrow constriction forms a structural determinant of the Mg^{2+} block (Burnashev et al., 1992b; Mori et al., 1992; Sakurada et al., 1993). The critical blocking site for extracellular Mg^{2+} is formed by the N-site and N+1 site of the NR2 subunit, and the contribution to the blocking site is stronger for the N+1 site than for the N-site asparagine. Much of the voltage dependence of the block is an intrinsic, local property of NR2 subunits at the narrow constriction. The N-site asparagine of the NR1 subunit contributes only little to the block by extracellular Mg^{2+} (Wollmuth et al., 1998a), but it represents the dominant blocking site for intracellular Mg^{2+}. The physiological function of the block by intracellular Mg^{2+} is unknown (Wollmuth et al., 1998b). In the following, only the block by extracellular Mg^{2+} will be considered.

Subtype-specific differences of Mg^{2+} block are determined by the NR2 subunit. Channels containing NR2A and NR2B are more sensitive to Mg^{2+} block compared to NR2C- or NR2D-containing channels (Monyer et al., 1994). Consequently, currents mediated by NR1/NR2A and NR1/NR2B channels are more strongly reduced by Mg^{2+} than currents mediated by NR1/NR2C and NR1/NR2D channels, predominantly reflecting a difference in voltage dependence. These subtype-specific differences of Mg^{2+} block are determined by at least three amino acid clusters of

the NR2 subunit, likely to be positioned close to the channel pore (Kuner and Schoepfer, 1996).

1.3.5 Kinetic properties of NMDA receptors

Compared to non-NMDARs, NMDARs display high affinity to glutamate (McBain and Mayer, 1994) and activate and deactivate much slower: they open at least one order of magnitude more slowly (∼10 ms) and remain active for a long time (50-500 ms), even when glutamate has already been removed from the synaptic cleft (∼1 ms, Clements et al., 1992). For full receptor activation, NMDARs require binding of two molecules of glutamate and two molecules of the coagonist (Benveniste and Mayer, 1991; Clements and Westbrook, 1991). The deactivation time course of these receptors is much longer than the dwell time of glutamate in most synaptic clefts (Clements et al., 1992), and therefore determines the EPSC duration. NMDAR currents decay with biphasic kinetics, meaning that the decay is composed of a slow and a fast component (Lester et al., 1990). The underlying kinetics of NMDAR gating responsible for the slow NMDA EPSC time course are extremely complex. To understand and describe the parameters determining the shape of NMDAR responses including activation, deactivation, and desensitization, different single-channel models have been developed considering different states (conducting and nonconducting) as well as distinct activity patterns (kinetic modes) of the receptor (Lester and Jahr, 1992; Popescu and Auerbach, 2004). The hypothesis that the NMDAR decay kinetics are controlled by the unbinding rate of transmitter has been supported by different studies (Colquhoun et al., 1977; Pan et al., 1993), but more recently it has been proposed that the slow NMDAR-mediated current decay does not arise from slow agonist dissociation per se, but rather mainly from slow and frequent oscillations between fully liganded open and closed conformations (Popescu and Auerbach, 2003). In addition, it has been suggested that the biphasic decay largely reflects modal gating and that desensitization has only a minor role (Zhang et al., 2008).

The deactivation of NMDARs is dependent on the subunit composition. Deactivation times are quite distinct for the diheteromeric NMDAR subtypes and span a ∼50-fold range, exhibiting following order from the fastest to the slowest

decay: NR2A < NR2B = NR2C ≪ NR2D (Cull-Candy and Leszkiewicz, 2004; Vicini et al., 1998). The developmental change of subunit expression in the brain (see section 1.3.3) is often described to be related to changes in the NMDA EPSC decay (Cull-Candy et al., 2001).

NMDARs desensitize in the continued presence of agonist: transmitter molecules are bound with high affinity, but the channel remains closed. The desensitization is slow and complex and involves at least three distinct processes (McBain and Mayer, 1994). It has been described that NMDAR responses desensitize due to a rise in intracellular Ca^{2+} resulting from influx through NMDARs; this form is referred to as Ca^{2+}-dependent desensitization (Legendre et al., 1993; Vyklický, 1993; Zorumski et al., 1989). The glycine-dependent form of desensitization seems to underlie the allosteric coupling of the glutamate- and glycine-binding sites, so that binding of glutamate decreases the affinity for glycine (Benveniste et al., 1990; Mayer et al., 1989a). The third form of NMDAR desensitization is Ca^{2+}- and glycine-independent (Sather et al., 1992, 1990). Similar to the deactivation, all forms of desensitization are subunit-dependent. The combination of agonist and coagonist binding, opening and closing, transient Mg^{2+} block, desensitization, and agonist/coagonist unbinding determine the characteristic time course of NMDA EPSCs during a synaptic event.

1.3.6 Modulation of NMDA receptor function

The NMDAR channel function can be modulated by various endogenous and exogenous agents (McBain and Mayer, 1994). The main endogenous modulators are Zn^{2+}, protons, and polyamines (Dingledine et al., 1999).

Although the exact concentration of Zn^{2+} in the brain and especially within the synaptic cleft is still controversial, it is clear that Zn^{2+} represents an important modulator of NMDAR function (Smart et al., 2004) that is localized in synaptic vesicles at presynaptic glutamatergic terminals (Salazar et al., 2005). Zn^{2+} at low micromolar concentrations was found to inhibit NMDAR responses (Peters et al., 1987; Westbrook and Mayer, 1987). It turned out that this inhibition occurs by a voltage-independent, allosteric (non competitive) mechanism and appears as a decrease in the channel open probability (Christine and Choi, 1990; Legendre

and Westbrook, 1990; Mayer et al., 1989b). At concentrations >20 μM, Zn^{2+} inhibits NMDARs by a voltage-dependent mechanism, probably by binding the same residues inside the pore that are important for Mg^{2+} block (Christine and Choi, 1990; Legendre and Westbrook, 1990; Mayer et al., 1989b; Paoletti et al., 1997). However, strength and voltage dependence of Zn^{2+} block is weaker compared to Mg^{2+} block, presumably because of an easier permeation of Zn^{2+} than Mg^{2+} into the channel pore (Christine and Choi, 1990; Legendre and Westbrook, 1990; Mayer et al., 1989b; Paoletti et al., 1997). While the voltage-dependent Zn^{2+} sensitivity is similar for all NMDAR subtypes, the voltage-independent Zn^{2+} sensitivity was shown to be subunit-dependent. NR2A-containing NMDARs have a much higher Zn^{2+} sensitivity than all other NMDAR subtypes, being already inhibited in the low nanomolar range, NR2B-containing receptors instead are only inhibited in the low micromolar range (Paoletti et al., 1997; Traynelis et al., 1998). The NR2A-specific Zn^{2+} inhibition is not complete, with 20-40% of the maximal NMDAR current remaining (Chen et al., 1997; Paoletti et al., 1997). The NTD of the NR2A and NR2B subunit form the Zn^{2+} binding site with different affinities. In addition to the NR2 subunit dependence, Zn^{2+} inhibition is influenced by NR1 splice variants (Paoletti et al., 1997; Traynelis et al., 1998) and the NR1 subunit might also participate in Zn^{2+} binding.

In the mammalian brain, the pH is highly dynamic and changes during synaptic transmission, glutamate receptor activation, glutamate uptake as well as under pathological situations (Amato et al., 1994; Chesler, 1990; Chesler and Kaila, 1992). It influences glutamate receptor function, which becomes particularly obvious by the inhibition of NMDARs by physiologically relevant concentrations of protons: the IC_{50} value for proton inhibition corresponds to pH 7.3, so that the receptor is tonically inhibited ($\sim$50%) at physiological pH (Traynelis and Cull-Candy, 1990). The inhibition occurs through reduction of the single-channel opening frequency without affecting open time and conductance (McBain and Mayer, 1994). The acidification under pathological conditions causes stronger inhibition of NMDARs and therefore minimizes their contribution to neurotoxicity (Kaku et al., 1993; Tombaugh and Sapolsky, 1993). Like voltage-independent Zn^{2+} inhibition, NMDAR inhibition by protons is influenced by the NR2 subunit and NR1 splice variants. Residues influencing pH sensitivity are found on both NR1 and

NR2 subunits (Gallagher et al., 1997; Kashiwagi et al., 1997). The physical location of the proton sensor responsible for proton inhibition within the NMDAR is still unknown, but mutagenesis studies of NMDAR subunits suggest that residues within the linker regions connecting the NTD to the transmembrane pore-forming elements contribute to proton-sensitive channel gating (Low et al., 2000; Zheng et al., 2001). It has also been suggested that there is a tight coupling of the proton sensor and gating (Kashiwagi et al., 1997; Traynelis et al., 1998).

Endogenous polyamines such as spermine or spermidine have complex effects on NMDARs. At least three different effects of extracellular polyamines have been described: voltage-dependent inhibition, glycine-dependent potentiation, and voltage- and glycine-independent potentiation of NMDARs (Rock and Macdonald, 1995; Williams, 1997). The voltage-dependent inhibition involves similar residues as Mg^{2+} and Zn^{2+} block inside the channel pore (Kashiwagi et al., 1997) and is dependent on the NR2 subunit. Similar to Mg^{2+}, it is due to fast-channel block, but of lower affinity and therefore likely negligible under physiological conditions (Williams, 1997). Other inhibitory effects may involve a decrease in the affinity for glutamate (Williams, 1994). Both glycine-dependent and glycine-independent polyamine potentiation of NMDAR function are influenced by the NR2 subunit. Glycine-dependent potentiation occurs at NR2A- and NR2B-containing receptors (Williams, 1994; Zhang et al., 1994) and is not influenced by NR1 splice variants (Durand et al., 1993). It involves an increase in channel opening frequency and decrease of desensitization of NMDARs, probably reflecting relief of tonic proton inhibition (Benveniste and Mayer, 1993; Lerma, 1992; Rock and Macdonald, 1992; Traynelis et al., 1995). In contrast, glycine-independent potentiation is described only for NR2B-containing receptors and is influenced by NR1 RNA splicing (Durand et al., 1993; Williams, 1994; Zhang et al., 1994). This form of polyamine potentiation involves an increase in the affinity of NMDARs for glycine (Benveniste and Mayer, 1993; McGurk et al., 1990).

1.3.7 Pharmacology of NMDA receptor subtypes

Numerous NMDAR antagonists have been developed to study NMDAR functions, but pharmacological tools discriminating between NMDAR subtypes remain lim-

ited. Three major classes of NMDAR antagonists can be distinguished on the basis of their mechanism of antagonism: (1) Competitive NMDAR antagonists act at the agonist or coagonist binding domains, (2) NMDAR channel blockers block the pore after channel activation, and (3) non-competitive allosteric NMDAR antagonists act at extracellular domains (Fig. 3).

The first NMDAR antagonists were competitive antagonists acting on the glutamate binding site of the NR2 subunit. One of the first compounds discovered was (D)-2-amino-5-phosphonopentanoate (D-AP5; Davies et al., 1981), which is still widely used because it displays strong preference for NMDARs over all other iGluRs. Competitive antagonists (D-AP5, D-AP7, D-CPP) show some selectivity between the different NR2 subunits (affinity ranking typically NR2A > NR2B > NR2C > NR2D), but the affinity differences are smaller than 10-fold and consequently do not allow selective inhibition of a particular receptor subtype (Feng et al., 2005). A more recent competitive antagonist, the Novartis compound NVP-AAM077, has enhanced selectivity for NR1/NR2A over NR1/NR2B receptors. However, its selectivity has been overestimated, because the 100-fold difference in affinity for NR1/NR2A over NR1/NR2B recombinant human receptors expressed in oocytes (Auberson et al., 2002; Liu et al., 2004) turned out to be only 12-fold for the respective recombinant rodent receptors (Berberich et al., 2005; Feng et al., 2004; Weitlauf et al., 2005). In addition, it also antagonizes NR2C- and NR2D-containing receptors (Feng et al., 2004).

The second class of antagonists inhibits NMDARs by occluding the ion channel pore. These channel blockers are uncompetitive antagonists and require receptor activation, i.e. channel opening, in order to bind within the channel pore. Channel blockers like phencyclidine (PCP), ketamine, memantine, and amantadine discriminate only poorly between NMDARs subtypes (Bresink et al., 1996; Yamakura et al., 1993), and also the highly selective NMDAR channel blocker dizolcipine (MK-801) which is more potent at inhibiting NR1/NR2A and NR1/NR2B receptors than NR1/NR2C and NR1/NR2D receptors has a less than 10-fold difference in affinity (Yamakura et al., 1993).

In addition to Zn^{2+} that is an endogenous subunit-specific allosteric NMDAR modulator, synthetic organic inhibitors with subtype selectivity have been developed. Ifenprodil was discovered to display strong (>200-fold) selectivity for NR2B-

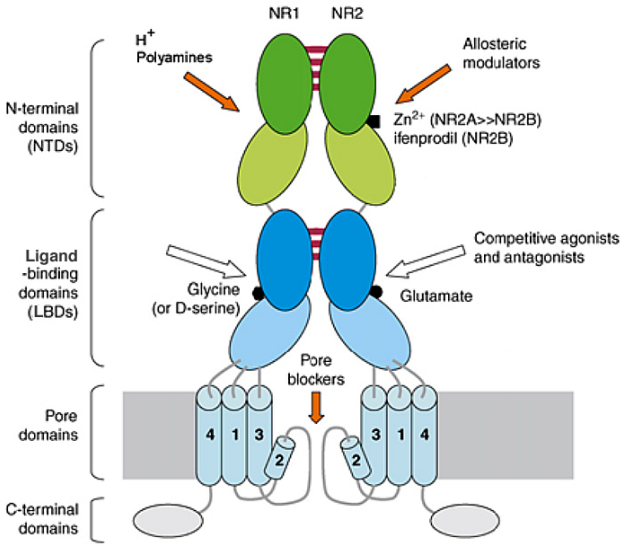

Fig. 3: Potential ligand binding sites at NMDARs. For clarity, only one of the two NR1/NR2 heterodimers is shown. The NR2 LBD binds glutamate, the NR1 LBD binds the coagonist. White arrows indicate binding sites for competitive agonists and antagonists. Thick orange arrows indicate sites that bind allosteric modulators (e.g. Zn^{2+} or ifenprodil and derivatives), acting as non-competitive antagonists. Pore blockers (e.g. Mg^{2+} or MK-801) bind in the ion channel pore (adapted and modified from Paoletti and Neyton, 2007).

containing receptors (Williams, 1993). Because of the poor selectivity of ifenprodil concerning other classes of receptors like e.g. alpha-adrenergic and serotoninergic receptors, derivatives with higher selectivity have been developed. Such derivatives like Ro25-6981 and CP-101,606 show even higher selectivity (up to 3000-fold difference) for the NR2B-subunit compared to ifenprodil (Fischer et al., 1997; Mott et al., 1998). Ifenprodil and derivatives are allosteric NMDAR inhibitors with selectivity for the NR2B subunit (Williams, 1993) and inhibit NR2B-containing receptors by a non-competitive and voltage-independent mechanism. Ifenprodil and derivatives bind to the NR2B-NTD (Gallagher et al., 1996; Perin-Dureau et al., 2002) and inhibit the NMDAR by increasing the sensitivity of the receptor to negative modulation by protons, thus enhancing tonic inhibition at physiological pH (Mott et al., 1998). Due to their subtype selectivity, ifenprodil and its derivatives seem to be convenient tools to decipher NMDAR subtype-specific roles. However, difficulties arising from the coexistence of di- and triheteromeric NR2B-containing receptors as well as drug-specific properties have to be considered when relating drug effects to specific NMDAR subtypes and will be described and discussed in detail later.

1.3.8 NMDA receptors and disease

Inappropriate activation of NMDARs has been implicated in the etiology of a range of acute and chronic neurodegenerative disorders (e.g. hypoxic-ischaemic injury, occuring after stroke or brain trauma, Parkinson, Huntington, Alzheimer, and epilepsy). Excessive Ca^{2+} influx through NMDARs can cause excitotoxic neuronal death, and thus, blockade of NMDARs was shown to be neuroprotective in animal models of stroke and epilepsy (Lee et al., 1999), turning modulators of NMDAR function into promising therapeutic targets for the treatment of many brain disorders. However, the usefulness of non-selective NMDAR antagonists was limited because of intolerable side effects (e.g. hallucinations, memory, and motor deficits), partly arising by their action on normal synaptic transmission. Therefore, blockade of excessive NMDAR activity has to be achieved without interference with physiological activity. The lack of discrimination between the different NMDAR subtypes is considered as one explanation for the failures of the first-generation NMDAR antagonists in clinical trials. Subunit-selective NMDAR antagonists have an improved side effect profile compared to the broad-spectrum antagonists. Ifenprodil and derivatives are attractive for clinical use for two reasons: first, the NR2B-directed antagonists are relatively well tolerated and second, they are maximally active at persistently activated NMDARs and at acidic pH (activity and pH dependence; Kew et al., 1996; Mott et al., 1998), conditions that often occur in pathological situations. Although NR2B-directed NMDAR antagonists show good efficacy as neuroprotectants and/or analgesics in various animal models (Chizh and Headley, 2005), none of them has yet completed clinical trials and developed into an approved drug because of emerging side effects in recent clinical studies (e.g. see Chaperon et al., 2003; Nicholson et al., 2007). In contrast, the low affinity, broad-spectrum NMDAR channel blocker memantine has been approved for the treatment of moderate to severe Alzheimer's disease. Memantine is thought to mediate its beneficial effects by normalizing aberrant, disease-associated NMDAR activation without affecting physiological activity. Its exceptional clinical tolerance might be due to its low affinity binding to open channels and its relatively fast unblocking kinetics (Johnson and Kotermanski, 2006; Lipton, 2006).

Hypofunction of NMDARs may be related to some human cognitive disorders,

in particular schizophrenia. Non-selective NMDAR channel blockers like PCP or ketamine disrupt memory function and cause a schizophrenia-like phenotype in healthy humans (Tsai and Coyle, 2002). Reduced NMDAR expression or impaired NMDAR function in transgenic mice leads to schizophrenia-related behaviours (Ballard et al., 2002; Mohn et al., 1999). Thus, positive modulators might represent a strategy to enhance NMDAR function under pathological conditions of receptor hypofunction, but should exclude the triggering of excitotoxicity through receptor overactivation. To date, enhancing NMDAR function under pathological conditions of NMDAR hypofunction is tried to be achieved by enhancing the glycine site occupancy, and these studies have yielded encouraging preliminary data (Javitt, 2008).

1.4 Hippocampus

An excellent framework to study NMDAR-related questions is the hippocampus. The hippocampus plays important roles in long-term memory, in particular episodic and semantic memory, and spatial navigation. It is a paired structure and located bilaterally in the medial temporal lobe of the brain. The hippocampus belongs to the limbic system and has the shape of a curved tube. The hippocampal subregions CA1 to CA3 and their neighbouring regions, the dentate gyrus, subiculum and entorhinal cortex, are collectively termed the 'hippocampal formation'. Its functional organization has traditionally been described as trisynaptic circuit, containing three major afferent pathways appearing as three excitatory synapses in series (Fig. 4): (1) The medial and lateral perforant-path (MPP and LPP) arising from the entorhinal cortex (EC) project to granule cells of the dentate gyrus (DG) and to pyramidal cells in CA3, CA1, and subiculum (Sb). The perforant path is considered to be the major input to the hippocampus. (2) The axons of DG granule cells, termed mossy fibers, innervate pyramidal cells in CA3. (3) Axons of the CA3 pyramidal cells, termed Schaffer collaterals, project to CA1 pyramidal cells. CA3 pyramidal cells can also form synapses with CA1 pyramidal cells from the contralateral hippocampus. The principal output from the hippocampus is formed by the pathway from CA1 to the subiculum and to the EC. Besides the EC input the hippocampus receives further input from the medial septum, the brainstem,

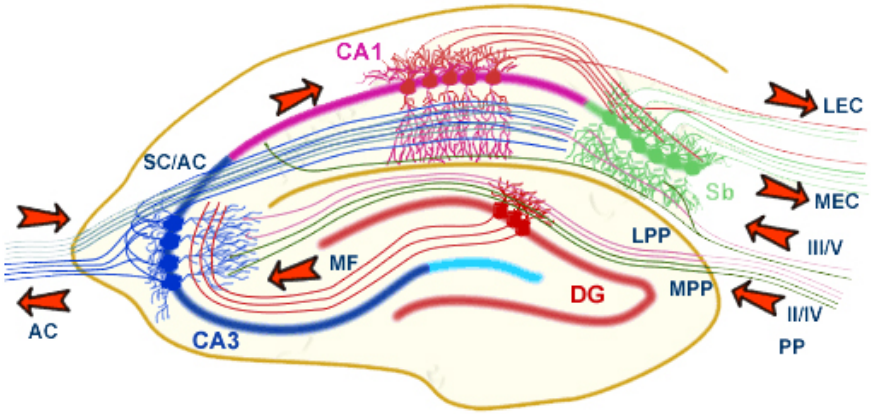

Fig. 4: The hippocampal network. The hippocampus forms a principally unidirectional network, with input from the entorhinal cortex (EC) that projects to the dentate gyrus (DG) and pyramidal cells via the perforant path (PP - split into lateral and medial). The mossy fiber (MF) pathway connects the granule cells to the CA3 pyramidal cells. CA3 neurons send axons to CA1 pyramidal cells via the Schaffer collateral pathway (SC), as well as to CA1 in the contralateral hippocampus via the associational commissural pathway (AC). CA1 neurons send axons to the subiculum (Sb) and to the EC. The main hippocampal output from CA1 and Sb goes to the lateral EC (LEC) and medial EC (MEC) (adapted from Collingridge G., MRC laboratory, Bristol).

hypothalamus, thalamus, and amygdala.

The hippocampus is organized in three layers: the polymorphic layer (stratum oriens), the pyramidal layer (stratum pyramidale), and the molecular layer (stratum radiatum and stratum lacunosum moleculare).

1.5 Aim of the project

Diheteromeric NR1/NR2 receptors have been extensively studied in heterologous systems and in cultured neurons, leading to the identification of NR2 subunit-specific synthesis, trafficking, and degradation pathways (Yashiro and Philpot, 2008). In contrast, NR2 subunit-specific roles in the induction of synaptic plasticity (Collingridge et al., 2004) or excitotoxicity (Liu et al., 2007; Martel et al., 2009; von Engelhardt et al., 2007) remain inconclusive, especially in neuronal preparations, which contain di- and triheteromeric NMDARs (Al-Hallaq et al.,

2007; Brickley et al., 2003; Chazot et al., 1994; Kew et al., 1998; Luo et al., 1997; Sheng et al., 1994; Tovar and Westbrook, 1999). Presence of two different NR2 subunits within triheteromeric NMDARs could lead to unique receptor properties expanding the repertoire of diheteromeric NMDAR signaling. The difficulty to isolate triheteromeric NMDARs leaves their abundance, properties, and function ambiguous.

Expression of NR2A and NR2B in adult CA1 pyramidal cells leads to the formation of NR1/NR2A, NR1/NR2B, and NR1/NR2A/NR2B receptors (Al-Hallaq et al., 2007; Chazot et al., 1994; Kew et al., 1998; Luo et al., 1997; Sheng et al., 1994). The aim of this study was to decipher the synaptic NMDAR composition in CA1 neurons and to explore whether NR1/NR2A/NR2B receptors contribute to synaptic transmission. In order to find a signature of NR1/NR2A/NR2B receptors in CA3-to-CA1-synapses by whole-cell patch-clamp recordings, we analyzed subtype-specific characteristics of diheteromeric NMDARs in acute slices of mice in which either NR2A was constitutively ablated ($NR2A^{-/-}$, Sakimura et al., 1995), or NR2B was selectively removed from principal forebrain neurons ($NR2B^{\Delta Fb}$, von Engelhardt et al., 2008). These subtype-specific characteristics were compared to characteristics found in age-matched wild-type mice (WT), which express triheteromeric NMDARs in addition to the two diheteromeric NMDAR subtypes. This approach combined with the use of pharmacology in wild-type mice allowed us to estimate the NR1/NR2A/NR2B receptor proportion of the total NMDAR population in the hippocampus and may help to identify NMDAR subtypes in other brain regions.

2 Results

2.1 Sensitivity of NMDA EPSCs to extracellular Mg^{2+}

2.1.1 Mg^{2+} sensitivity of NMDA EPSC amplitudes

Agonist evoked currents mediated by recombinant NR1/NR2A receptors deactivate 3-4-fold faster than those mediated by recombinant NR1/NR2B receptors (Dingledine et al., 1999), while their sensitivity to extracellular Mg^{2+} is similar (Kuner and Schoepfer, 1996; Monyer et al., 1994). We performed whole-cell patch-clamp recordings in order to investigate the sensitivity to Mg^{2+} for different synaptic NMDAR subtypes in acute hippocampal slices. We stimulated the Schaffer collaterals and compared the amplitudes of NMDA EPSCs recorded at -40 and $+40$ mV in hippocampal CA1 neurons before and after washout of external Mg^{2+}. Diheteromeric NR1/NR2B receptors were investigated in $NR2A^{-/-}$ mice (Sakimura et al., 1995), and diheteromeric NR1/NR2A receptors in conditional $NR2B^{\Delta Fb}$ mice (von Engelhardt et al., 2008) to avoid perinatal lethality from complete NR2B knockout (Kutsuwada et al., 1996). Di- and triheteromeric NMDARs were investigated in age-matched wild-type mice (WT).

In $NR2B^{\Delta Fb}$ mice, NR2B is progressively removed over the first three postnatal months from principal forebrain neurons, including CA1 pyramidal cells. In 36 of 79 CA1 neurons recorded in P44 $NR2B^{\Delta Fb}$ mice, NMDA EPSCs had significantly shorter decay times than in wild-type mice and were unaffected by the NR2B-directed NMDAR antagonist CP-101,606 (10 μM; not shown), indicating the absence of NR2B subunits; thus NMDA EPSCs were mediated exclusively by NR1/NR2A receptors in these cells. A subset of the 36 cells was used for this project (Table 1).

Each mutant mouse line was compared to wild type at the respective age ($NR2A^{-/-}$ mice at P28; see Fig. 5A and 6A, B left panels, and $NR2B^{\Delta Fb}$ mice at

P44; see Fig. 5B and 6A, B right panels). For all three genotypes, Mg^{2+} washout similarly increased the amplitudes of NMDA EPSCs at −40 mV 3-4-fold (P28 and P44, $p > 0.05$), whereas changes of amplitudes at +40 mV were negligible and not different within each age group (P28 and P44, $p > 0.05$) (Fig. 5 A, B).

Thus, the sensitivity to Mg^{2+} block is comparable for synaptic NMDARs of the three genotypes.

Table 1: Deactivation kinetics for NMDA EPSCs (ms) recorded in CA1 neurons of wild-type, *NR2A*$^{-/-}$ and *NR2B*$^{\Delta Fb}$ mice at −40 and +40 mV in presence and absence of Mg^{2+} at the indicated ages. For each condition, $^{\#}$ indicates significance following Mg^{2+} washout and † indicates significance between −40 and +40 mV. Compared with both NR2 mutants, NMDA EPSC decay time in wild type was intermediate and distinct ($p < 0.0001$). From P5 to P28/P44, decay time accelerated in wild type in presence ($p < 0.0001$) and absence of Mg^{2+} ($p < 0.05$). Number of cells is indicated in parenthesis.

genotype	membrane potential	1 mM Mg^{2+}		
		P5	P28	P44
WT	−40 mV	83±4.15 (17)	53±2.49 (21)	55±2.11 (16)
	+40 mV	229±17.12† (17)	123±5.32† (21)	113±2.70† (16)
NR2A$^{-/-}$	−40 mV	146±13.87 (18)	233±18.60 (9)	
	+40 mV	303±23.73† (18)	307±16.18† (9)	
NR2B$^{\Delta Fb}$	−40 mV			25±1.20 (9)
	+40 mV			52±2.94† (9)

genotype	membrane potential	0 mM Mg^{2+}		
		P5	P28	P44
WT	−40 mV	128±5.02$^{\#}$ (14)	100±8.49$^{\#}$ (21)	94±7.27$^{\#}$ (16)
	+40 mV	218±18.77† (12)	161±14.63$^{\#,\dagger}$(21)	131±6.23$^{\#,\dagger}$ (16)
NR2A$^{-/-}$	−40 mV	237±22.48$^{\#}$ (14)	306±16.64$^{\#}$ (9)	
	+40 mV	374±48.51† (14)	302±18.32 (9)	
NR2B$^{\Delta Fb}$	−40 mV			34±3.24$^{\#}$ (9)
	+40 mV			57±3.54† (9)

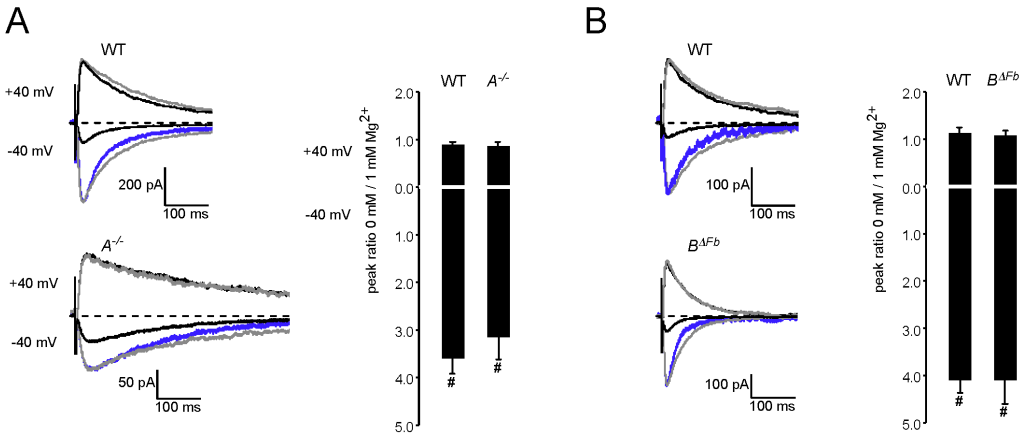

Fig. 5: Mg^{2+} sensitivity of amplitudes of NMDA EPSCs in wild-type, *NR2A*$^{-/-}$ and *NR2B*$^{\Delta Fb}$ mice. A, Left, representative averaged current traces before (black) and after (grey) Mg^{2+} washout for P28 wild-type and P28 *NR2A*$^{-/-}$ mice. Blue traces at −40 mV represent black traces scaled to the amplitude of grey traces. Bars show peak ratios, illustrating effects of Mg^{2+} washout on amplitudes of pharmacologically isolated (NBQX, 10 μM) NMDA EPSCs recorded in CA1 cells at −40 mV (downwards) and +40 mV (upwards). The basis of the bars at 0 is marked by a white line. At −40 mV, NMDA EPSCs increased 3.60 ± 0.33 -fold in P28 wild-type (n = 21, $^{\#}p < 0.0001$) and 3.16 ± 0.48 -fold in P28 *NR2A*$^{-/-}$ mice (n = 9, $^{\#}p < 0.001$). At +40 mV, NMDA EPSCs remained unchanged (WT, 0.89 ± 0.05, n = 21, p = 0.0497; *NR2A*$^{-/-}$, 0.86 ± 0.07, n = 9, p = 0.0804). **B**, same as **A**, but for P44 wild-type (n = 11) and P44 *NR2B*$^{\Delta Fb}$ mice (n = 7) at −40 mV (WT, 4.10 ± 0.29, $^{\#}p < 0.0001$; *NR2B*$^{\Delta Fb}$, 4.12 ± 0.51, $^{\#}p < 0.001$) and at +40 mV (WT, 1.12 ± 0.11, p = 0.1480; *NR2B*$^{\Delta Fb}$, 1.07 ± 0.09, p = 0.3433).

2.1.2 Mg^{2+} sensitivity of NMDA EPSC decay time

Consistent with recombinant diheteromeric NMDARs (Cull-Candy and Leszkiewicz, 2004; Monyer et al., 1994; Vicini et al., 1998), NR1/NR2B receptor-mediated NMDA EPSCs at CA1 synapses of *NR2A*$^{-/-}$ mice decayed significantly slower than NR1/NR2A receptor-mediated NMDA EPSCs in *NR2B*$^{\Delta Fb}$ mice (about 9-fold slower at −40 mV and about 6-fold slower at +40 mV; Fig. 6A, Table 1). This difference was observed in presence of Mg^{2+} as well as following washout of Mg^{2+}, which prolonged the decay time constants of NMDA EPSCs, consistent with previous findings (Konnerth et al., 1990). In wild-type mice, the decay time of NMDA EPSCs was distinct ($p < 0.0001$) and intermediate when compared with that in both NR2 mutant mouse lines. This intermediate decay phenotype in

wild type could be due to the coexistence of NR1/NR2A and NR1/NR2B receptors in hippocampal synapses and does not necessarily identify the contribution of NR1/NR2A/NR2B receptors.

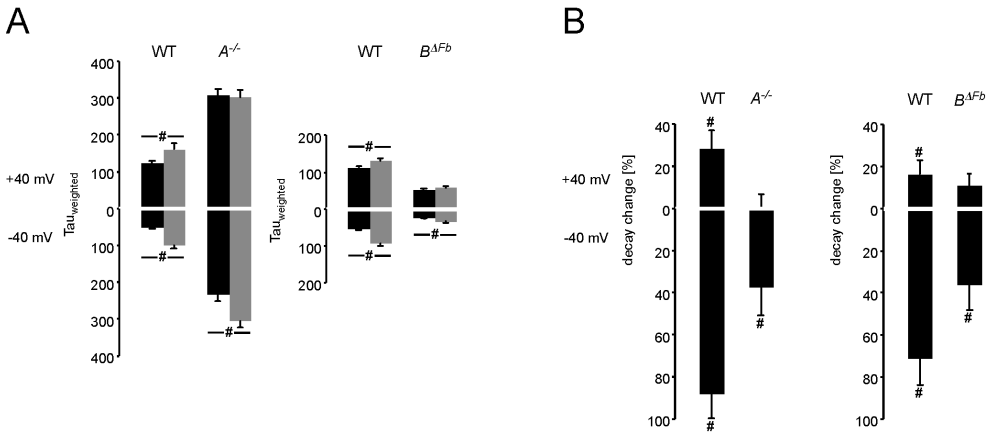

Fig. 6: Mg^{2+} sensitivity of deactivation kinetics of NMDA EPSCs in wild-type, *NR2A*$^{-/-}$ and *NR2B*$^{\Delta Fb}$ mice. See Fig. 5 for representative current traces. **A**, Averaged decay time constants ($Tau_{weighted}$) for P28 wild-type (n = 21) and *NR2A*$^{-/-}$ (n = 9) mice (left), and for P44 wild-type (n = 16) and *NR2B*$^{\Delta Fb}$ (n = 9) mice (right), in presence (black bars) and absence (grey bars) of Mg^{2+} at −40 mV (downwards) and +40 mV (upwards). Compared to wild type, NMDA EPSCs were slower in *NR2A*$^{-/-}$ mice and faster in *NR2B*$^{\Delta Fb}$ mice ($p < 0.0001$, respectively). At −40 mV, Mg^{2+} washout slowed down the decay time in all three genotypes, but at +40 mV only in wild type. For statistical comparison, see **B**. **B**, Changes of deactivation kinetics in % following Mg^{2+} washout for P28 wild-type (n = 21) and *NR2A*$^{-/-}$ (n = 9) mice (left) as well as for P44 wild-type (n = 16) and *NR2B*$^{\Delta Fb}$ (n = 9) mice (right). At −40 mV, decay changes were more pronounced in wild-type than in the two NR2 mutants (WT P28/P44, 88.24 ± 11.75% / 71.11 ± 12.99%, $^{\#}p < 0.0001$ / $^{\#}p < 0.0001$; *NR2A*$^{-/-}$, 37.47 ± 13.66%, $^{\#}p < 0.01$; *NR2B*$^{\Delta Fb}$, 36.50 ± 11.73%, $^{\#}p < 0.05$). At +40 mV, decay changes occured exclusively in wild type (WT P28/P44, 28.29 ± 8.55% / 16.34 ± 6.73%, $^{\#}p < 0.01$ / $^{\#}p = 0.0322$; *NR2A*$^{-/-}$, 0.60 ± 6.01%, $p = 0.7740$; *NR2B*$^{\Delta Fb}$, 11.01 ± 5.48%, $p = 0.1043$).

Notably, the NMDA EPSC decay time slowdown due to Mg^{2+} washout is more pronounced at negative than at positive membrane potentials in dentate gryrus granule cells (Konnerth et al., 1990). We also found this difference for NMDA EPSCs in CA1 synapses for all three genotypes, but to different extents. The slowdown of the NMDA EPSC decay time was more pronounced for wild-type than for both NR2 mutants at −40 mV (Fig. 6B). At +40 mV, the decay time of NMDA EPSCs slowed down only for wild-type mice, but remained unchanged for

NR2A$^{-/-}$ and *NR2B*$^{\Delta Fb}$ mice (Fig. 6; Table 1). Thus, removal of Mg^{2+} changed the deactivation kinetics of NMDA EPSCs at negative and positive potentials in wild type, but exclusively at negative potentials and to a lesser extent in both NR2 mutants. To our knowledge, this observation provides the first evidence that a population of NMDARs distinct from diheteromeric NR1/NR2A and NR1/NR2B receptors contributes to NMDA EPSCs in wild-type hippocampal slices.

2.2 Voltage dependence of NMDA EPSC decay time in adult wild-type mice and gene-targeted mouse lines

2.2.1 Voltage dependence of NMDA EPSC decay time in the presence of 1 mM Mg^{2+}

In wild-type mice, Mg^{2+} confers voltage dependence to the decay time of NMDA EPSCs, with slower kinetics at depolarized potentials (Hestrin, 1992). To estimate the voltage dependence of decay for NMDA EPSCs recorded in wild-type, *NR2A*$^{-/-}$ and *NR2B*$^{\Delta Fb}$ mice, we calculated the −40 mV/+40 mV ratio of the decay time constants. A small ratio reflects marked voltage dependence of decay. Fig. 7 shows the ratios for P28 only, because NMDA EPSCs were comparable in wild type at P28 and P44 (Figs. 5 and 6). In the presence of Mg^{2+}, NMDA EPSCs in *NR2A*$^{-/-}$ mice displayed a significantly reduced voltage dependence compared to wild-type and *NR2B*$^{\Delta Fb}$ mice (Fig. 7). Thus, Mg^{2+}-dependent voltage dependence was different for NR1/NR2A and NR1/NR2B receptors.

2.2.2 Voltage dependence of NMDA EPSC decay time in the absence of Mg^{2+}

Even in the absence of Mg^{2+}, NMDA EPSCs show voltage dependence and decay slower at depolarized than at more negative membrane potentials (Kirson and Yaari, 1996; Konnerth et al., 1990). As Mg^{2+} confers voltage dependence to the decay time of NMDA EPSCs, washout of Mg^{2+} increased the −40 mV/+40 mV

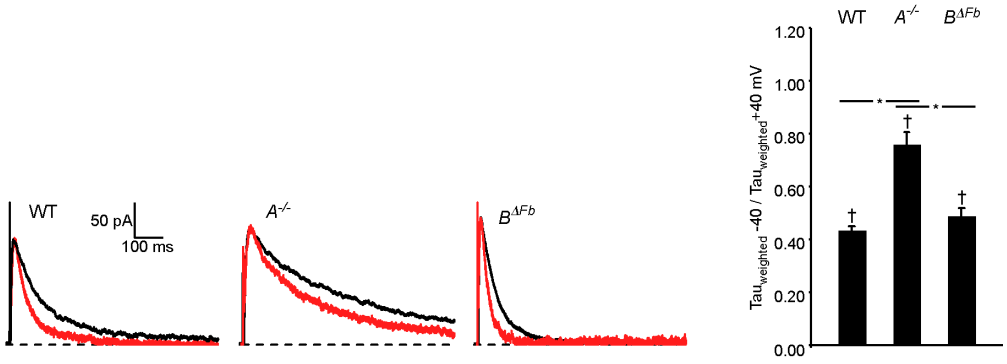

Fig. 7: Mg^{2+}-dependent voltage dependence of NMDA EPSC decay time in adult wild-type, *NR2A*$^{-/-}$ and *NR2B*$^{\Delta Fb}$ mice. Left panels, averaged representative current traces show NMDA EPSCs in the presence of 1 mM Mg^{2+} at +40 mV in black and NMDA EPSCs at −40 mV scaled to EPSCs at +40 mV in red. Right panel, the bar diagram shows the ratio of $Tau_{weighted}$ −40 / $Tau_{weighted}$ +40 mV in the presence of 1 mM Mg^{2+}. In all three genotypes, decay time was slower at +40 mV than at −40 mV (WT, 0.43 ± 0.02, n = 21, $^{\dagger}p < 0.0001$; *NR2A*$^{-/-}$, 0.76 ± 0.05, n = 9, $^{\dagger}p < 0.05$; *NR2B*$^{\Delta Fb}$, 0.49 ± 0.03, n = 9, $^{\dagger}p < 0.0001$). Voltage dependence of decay was reduced in *NR2A*$^{-/-}$ mice compared to wild-type and *NR2B*$^{\Delta Fb}$ mice (ANOVA, $^{*}p < 0.01$) and was similar in wild-type and *NR2B*$^{\Delta Fb}$ mice (ANOVA, p >0.05).

ratio of the decay time constants as expected. In the presence of Mg^{2+}, NMDA EPSCs in *NR2A*$^{-/-}$ mice displayed a significantly reduced voltage dependence compared to wild-type and *NR2B*$^{\Delta Fb}$ mice (Fig. 7). This genotypic difference was also observed in the absence of Mg^{2+}. NMDA EPSCs still decayed slower at positive than at negative potentials in wild-type and *NR2B*$^{\Delta Fb}$ mice, whereas the decay time of NMDA EPSCs in *NR2A*$^{-/-}$ mice was similar at −40 and +40 mV (Fig. 8). This demonstrates that voltage dependence of NMDA EPSCs was different for pure synaptic diheteromeric NMDARs in the presence as well as in the absence of Mg^{2+}.

Voltage dependence of NMDA EPSC decay in presence and absence of Mg^{2+} was similar for NR1/NR2A receptors in *NR2B*$^{\Delta Fb}$ mice and for the NMDARs in wild-type mice. Therefore, the absence of the distinct voltage dependence of decay for synaptic NR1/NR2B receptors in wild type let us conclude that NR1/NR2B receptors contribute to a minor extent to NMDA EPSCs in adult wild-type mice. In addition, the presence of a mixture of pure NR1/NR2A and NR1/NR2B receptors in wild-type synapses can be excluded, since we did not observe an intermediate

value for the voltage dependence of decay. In contrast, an intermediate value for NMDA EPSC decay time was observed in wild type compared to the two NR2 mutants (see chapter 2.1.2). Thus, synaptic triheteromeric NR1/NR2A/NR2B receptors mediate NMDA EPSCs with slower deactivation kinetics than diheteromeric NR1/NR2A receptors, but NR1/NR2A/NR2B and NR1/NR2A receptors display similar voltage dependence of decay.

In summary, our analysis of voltage dependence and decay time of NMDA EPSCs in three genotypes strongly suggests that NMDA EPSCs in adult CA3-to-CA1 synapses are mainly mediated by NR1/NR2A and NR1/NR2A/NR2B receptors.

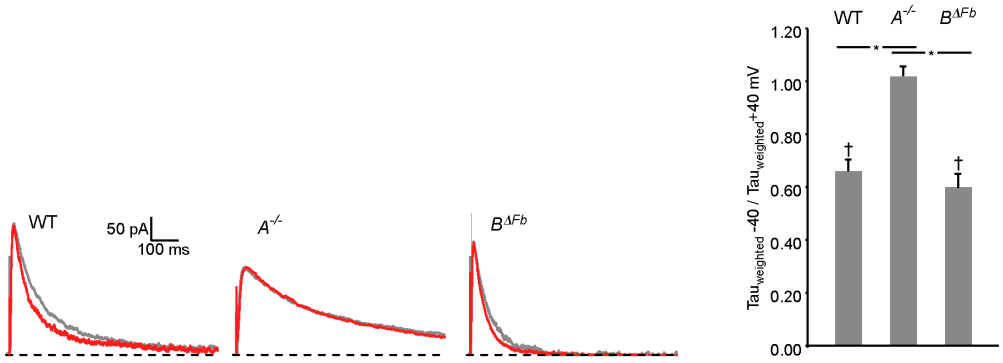

Fig. 8: Mg^{2+}-independent voltage dependence of NMDA EPSC decay time in adult wild-type, *NR2A*$^{-/-}$ and *NR2B*$^{\Delta Fb}$ mice. Left panels, averaged representative current traces show NMDA EPSCs in the absence of Mg^{2+} at +40 mV in grey and NMDA EPSCs at −40 mV scaled to EPSCs at +40 mV in red. Right panel, the bar diagram shows the ratio of $Tau_{weighted}$ −40 / $Tau_{weighted}$ +40 mV in the absence of Mg^{2+}. For wild-type and *NR2B*$^{\Delta Fb}$ mice, decay time was slower at +40 mV than at −40 mV, but similar at −40 mV and +40 mV for *NR2A*$^{-/-}$ mice (WT, 0.66 ± 0.04, n = 21, $^{\dagger}p < 0.001$; *NR2A*$^{-/-}$, 1.02 ± 0.03, n = 9, p = 0.94; *NR2B*$^{\Delta Fb}$, 0.60 ± 0.05, n = 9, $^{\dagger}p < 0.0001$). The Mg^{2+}-independent voltage dependence of decay in wild-type and *NR2B*$^{\Delta Fb}$ mice was different from *NR2A*$^{-/-}$ mice (ANOVA, $^{*}p < 0.01$).

2.3 Examination of the NMDA receptor composition in neonatal CA3-to-CA1 synapses

2.3.1 Voltage dependence of NMDA EPSC decay time in neonatal wild-type and *NR2A*$^{-/-}$ mice

Our experiments revealed a distinct voltage dependence of decay for NMDA EPSCs mediated via NR1/NR2B receptors in P28 *NR2A*$^{-/-}$ mice, that was not observed in CA1 neurons of adult wild-type mice (Figs. 7, 8). As NR2B expression is high at early postnatal stages when NR2A expression is still low (Monyer et al., 1994; Watanabe et al., 1993), we expected to find characteristics of NMDA EPSCs in neonatal wild-type similar to those in adult *NR2A*$^{-/-}$ mice (Figs. 7, 8). Indeed, the presence of NR1/NR2B receptors in P5 wild-type mice was suggested by a slowdown of NMDA EPSC decay time only at −40 mV caused by the Mg^{2+} washout similar to that observed for NR1/NR2B receptors in P28 *NR2A*$^{-/-}$ mice (P5 WT, −40 mV, 53.01 ± 10.53%, n = 14; $p < 0.0001$; +40 mV, 0.10 ± 10.95%, n = 12; $p > 0.05$; P28 *NR2A*$^{-/-}$, −40 mV, 37.47 ± 13.66%, n = 9, $p < 0.01$; +40 mV, 0.60 ± 6.01% n = 9; $p > 0.05$; Fig. 6B and Table 1). Similarly, the voltage dependence of NMDA EPSC decay should be less pronounced in neonatal than adult wild-type mice. However, voltage dependence of NMDA EPSC decay in neonatal wild-type mice was not different from that in adult wild-type mice (1 mM and 0 mM Mg^{2+}, $p > 0.05$; Figs. 7 and 8 vs. Fig. 9), and for both developmental stages, it was more pronounced than in adult *NR2A*$^{-/-}$ mice (1 mM Mg^{2+}, $p < 0.0001$; 0 mM Mg^{2+}, $p < 0.01$; Figs. 7 and 8 vs. Fig. 9). These observations indicate that voltage dependence of NMDA EPSC deactivation remains constant over development in wild-type mice, which may be accomplished by NR2 subunits in addition to NR2B.

To check whether NR2A-containing NMDARs could be present in neonatal wild-type synapses and contribute to the observed voltage dependence of NMDA EPSCs, we investigated NMDA EPSCs in neonatal *NR2A*$^{-/-}$ mice. Surprisingly, compared to adult *NR2A*$^{-/-}$ mice, NMDA EPSCs recorded in neonatal exhibited

stronger voltage dependence of NMDA EPSC decay time in presence and absence of Mg^{2+} ($p < 0.001$ for 1 and 0 mM Mg^{2+}; Figs. 7 and 8 vs. Fig. 9). Furthermore, the voltage dependence of NMDA EPSC deactivation recorded in neonatal wild-type and neonatal *NR2A*$^{-/-}$ mice was comparable (1 mM and 0 Mg^{2+}, $p > 0.05$; Fig. 9). Thus, early NR2A expression in hippocampal synapses is not the reason for the stronger voltage dependence of NMDA EPSC decay time in neonatal wild-type compared with adult *NR2A*$^{-/-}$ mice.

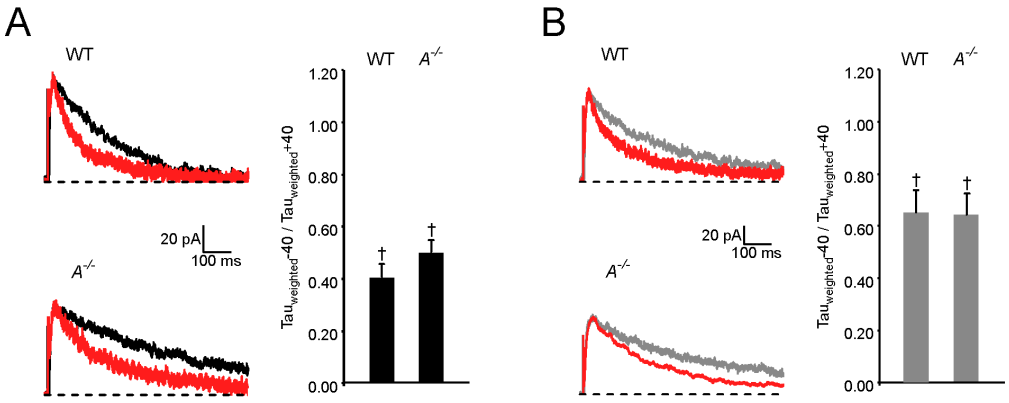

Fig. 9: Voltage dependence of NMDA EPSC deactivation kinetics in neonatal wild-type and *NR2A*$^{-/-}$ mice. Averaged representative current traces show NMDA EPSCs at +40 mV in black (**A**, normal Ringer solution containing 1 mM Mg^{2+}) and in grey (**B**, Mg^{2+}-free Ringer solution), and NMDA EPSCs at −40 mV scaled to EPSCs at +40 mV in red. **A**, The bar diagram shows the ratio $Tau_{weighted}$ −40 / $Tau_{weighted}$ +40 mV in presence of 1 mM Mg^{2+}. For wild-type and *NR2A*$^{-/-}$ mice, decay time was slower at +40 mV than at −40 mV and not different from each other ($p = 0.1799$; WT, 0.41 ± 0.05, n = 17, $^{\dagger}p < 0.0001$; *NR2A*$^{-/-}$, 0.50 ± 0.05, n = 18, $^{\dagger}p < 0.0001$). **B**, same as **A**, but in the absence of Mg^{2+}. Neonatal wild-type and *NR2A*$^{-/-}$ mice showed similar Mg^{2+}-independent voltage dependence of decay ($p = 0.7065$; WT, 0.65 ± 0.09, n = 12, $^{\dagger}p < 0.0001$; *NR2A*$^{-/-}$, 0.69 ± 0.06, n = 14, $^{\dagger}p < 0.01$).

2.3.2 Effect of CP-101,606 on NMDA EPSCs in neonatal and adult *NR2A*$^{-/-}$ mice

Instead of NR2A expression, the stronger voltage dependence of NMDA EPSC decay time in neonatal versus adult *NR2A*$^{-/-}$ mice might arise from NR2D expression in young hippocampal synapses (Monyer et al., 1994). Because antagonists for

NR1/NR2D receptors have poor subtype selectivity (Feng et al., 2004; Paoletti and Neyton, 2007), we compared the effect of CP-101,606 (10 μM), an NR2B-directed NMDAR antagonist, in neonatal and adult *NR2A*$^{-/-}$ mice. If NR2D was present additionally to NR2B in neonatal CA3-to-CA1 synapses of *NR2A*$^{-/-}$ mice and decreases over development, the reduction of NMDA EPSCs by CP-101,606 should be smaller in neonatal than in adult *NR2A*$^{-/-}$ mice. However, NMDA EPSCs were reduced to similar extents in neonatal and adult *NR2A*$^{-/-}$ mice (Fig. 10), arguing against the presence of NR1/NR2D receptors in synapses of neonatal CA1 pyramidal cells.

In summary, the voltage dependence of NMDA EPSC decay time in neonatal wild-type synapses cannot be caused by the presence of NR2A or by NR1/NR2D receptors, but rather by the presence of NR1/NR2B receptors displaying different voltage dependence of deactivation over development.

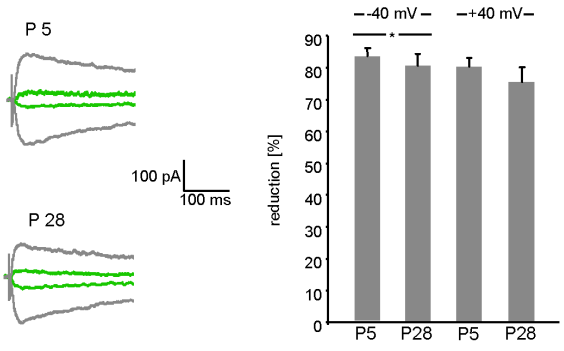

Fig. 10: Effect of CP-101,606 on NMDA EPSCs in neonatal and adult *NR2A*$^{-/-}$ mice. NMDA EPSCs were similarly reduced in neonatal and adult *NR2A*$^{-/-}$ mice (reductions in 0 mM Mg^{2+} and at −40 mV: P5, 83.30 ± 2.53%, n = 4; P28, 80.33 ± 3.83%, n = 7; p > 0.05, and at +40 mV: P5, 80.05 ± 2.62%, n = 4; P28, 75.13 ± 4.53% n = 7; p > 0.05).

2.4 Effects of NR2B-directed NMDA receptor antagonists on NMDA EPSCs during postnatal development

2.4.1 Effects of CP-101,606

Next, we combined the characterization of the NMDAR composition in wild-type synapses by subtype-specific kinetic properties deduced from NR2A and NR2B mutant mice (Figs. 6, 7, 8) with a pharmacological approach. The NR2B-directed

NMDAR antagonist CP-101,606 (10 μM) reduced NMDA EPSCs in the absence of Mg^{2+} in neonatal wild-type mice by about 65%, and at P28 by about 50% (Fig. 11A). Given that NR1/NR2B receptors appear to be a minor population in adult hippocampal synapses (Figs. 5-9), the 50% reduction by CP101-606 at P28 must result from antagonism of NR1/NR2A/NR2B rather than NR1/NR2B receptors. NR1/NR2A/NR2B receptors likely contribute to NMDA EPSCs more than 50%, because CP-101,606 (10 μM) antagonizes recombinant NR1/NR2B receptors in 0 mM Mg^{2+} only up to 80-90% (Mott et al., 1998; Williams, 1993).

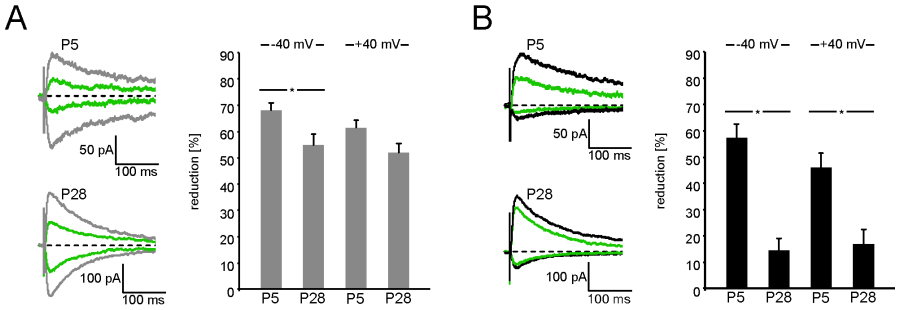

Fig. 11: Effects of CP-101,606 on NMDA EPSCs in neonatal versus adult wild-type mice. Averaged representative current traces show NMDA EPSCs at −40 and +40 mV in absence (**A**, grey) and presence (**B**, black) of Mg^{2+} before and after (green) perfusion of CP-101,606 (10 μM; 20 min). **A**, Reduction of NMDA EPSCs recorded at −40 and +40 mV by CP-101,606 in Mg^{2+}-free Ringer solution for P5 and P28 wild-type mice (P5, 68.18 ± 2.89% (n = 6) at −40 mV; 61.53 ± 2.80% (n = 6) at +40 mV; P28, 54.98 ± 4.08% (n = 9) at −40 mV and 52.0 ± 3.44% (n = 9) at +40 mV). From P5 to P28, the effect of CP-101,606 was significantly reduced at −40 mV ($^*p < 0.05$), but not at +40 mV (p = 0.0700). **B**, same as **A**, but in presence of 1 mM Mg^{2+} (P5, 57.47 ± 5.19% (n = 7) at −40 mV and 46.01 ± 5.35% (n = 7) at +40 mV; P28, 14.47 ± 4.45% (n = 7) at −40 mV and 17.0 ± 5.39% (n = 7) at +40 mV). The effect of CP-101,606 was significantly reduced from P5 to P28 (−40 mV, $^*p < 0.0001$; +40 mV, $^*p < 0.01$).

Previous studies demonstrated a developmental decrease in the sensitivity of NR2B-directed NMDAR antagonists in various brain regions (Barth and Malenka, 2001; Bellone and Nicoll, 2007; Brothwell et al., 2008; de Marchena et al., 2008; Lopez de Armentia and Sah, 2003), explained by a postnatal increase in NR2A expression (Monyer et al., 1994; Sans et al., 2000; Sheng et al., 1994). Under our experimental conditions in 0 mM Mg^{2+}, the sensitivity of CP-101,606 was only moderately reduced from P5 to P28 at −40 mV and did not change at +40 mV

(Fig. 11A). When repeating this experiment in presence of the physiological Mg^{2+} concentration (1 mM), sensitivity of CP-101,606 was significantly reduced from P5 to P28 (Fig. 11B), indicating that the recording conditions can influence the sensitivity of CP-101,606.

2.4.2 Effects of ifenprodil

In addition to CP-101,606, we also used ifenprodil (3 μM), another NR2B-directed NMDAR antagonist. Consistent with CP-101,606, the sensitivity of ifenprodil was not reduced from P5 to P28 in the absence, but in the presence of Mg^{2+} (Fig. 12A, B). At P28 and in presence of Mg^{2+}, NMDA EPSCs were not only less sensitive to ifenprodil compared to P5, but even increased (Fig. 12B; see also Kew et al., 1996). The currents were completely blocked by the NMDAR antagonist D-APV (50 μM; Fig. 12C), showing that the increased NMDA EPSCs after ifenprodil application were mediated by NMDARs.

In summary, presence or absence of Mg^{2+} influenced the sensitivity of CP-101,606 and ifenprodil. Notably, the strong peak reduction of NMDA EPSCs in absence of Mg^{2+} at P28 indicates that NR2B-containing NMDARs remain present in hippocampal synapses throughout postnatal development, reflecting a successive replacement of NR1/NR2B receptors by NR1/NR2A/NR2B receptors. Interestingly, even in cultured neurons, NR1/NR2A/NR2B receptors appear to be specifically targeted to, and incorporated into, nascent synapses (Tovar and Westbrook, 1999).

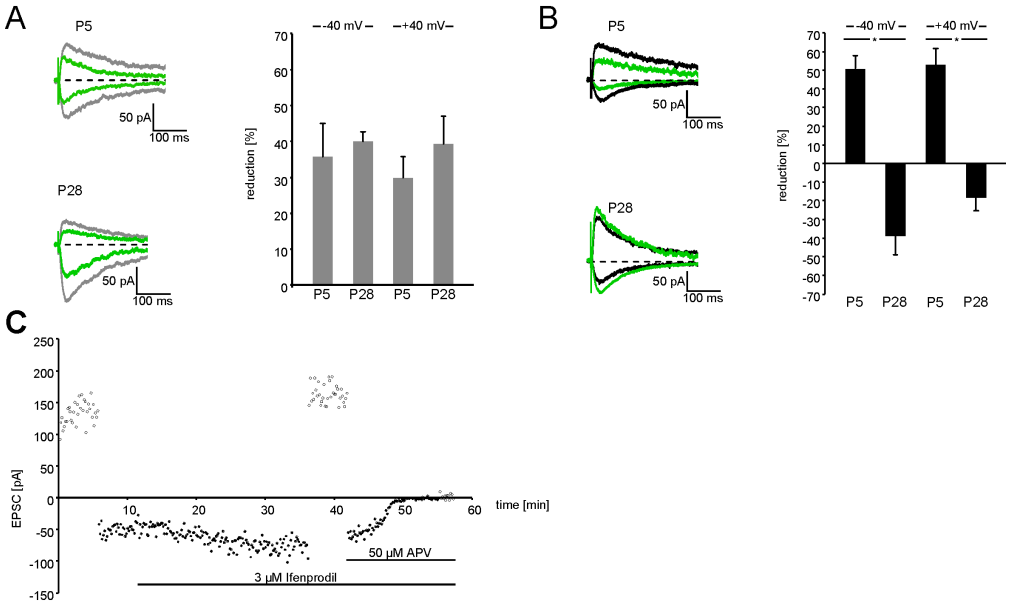

Fig. 12: Effects of ifenprodil on NMDA EPSCs in neonatal versus adult wild-type mice. Averaged representative current traces show NMDA EPSCs at −40 and +40 mV in absence (**A**, grey) and presence (**B**, black) of Mg^{2+} before and after (green) perfusion of ifenprodil (3 μM; 20 min). **A**, Reduction of NMDA EPSCs by ifenprodil in Mg^{2+}-free Ringer solution for wild-type mice (P5, 35.74 ± 9.25% (n = 6) at −40 mV and 29.94 ± 5.70% (n = 6) at +40 mV; P28, 40.03 ± 2.66% (n = 7) at −40 mV and 39.29 ± 7.52% (n = 7) at +40 mV). NMDA EPSCs were similarly reduced by ifenprodil in neonatal and adult wild-type mice (−40 mV, p = 0.6752; +40 mV, p = 0.3488). **B**, same as **A**, but in presence of 1 mM Mg^{2+} (P5, 50.70 ± 6.80% (n = 9) at −40 mV and 52.93% (n = 7) at +40 mV; P28, -38.86 ± 10.14% (n = 7) at −40 mV and -18.61 ± 6.69% (n = 7) at +40 mV). The effect of ifenprodil was significantly reduced from P5 to P28 ($p < 0.0001$). **C**, Time course of NMDA EPSC amplitudes recorded in 1 mM Mg^{2+} at +40 mV (open circles) and −40 mV (filled circles). NMDA EPSCs increased in the presence of ifenprodil (3 μM) and were subsequently blocked by D-APV (50 μM). Presence of antagonists is indicated by bars.

2.5 Effects of CP-101,606 on NMDA EPSCs in adult *NR2A*$^{-/-}$ mice

Recording conditions (absence versus presence of Mg^{2+}) influenced the sensitivity of CP-101,606 (Fig. 11). At P5, NMDA EPSCs showed a trend to be less inhibited in 1 than in 0 mM extracellular Mg^{2+} (−40 mV, $p > 0.05$; +40 mV, p = 0.05),

whereas at P28, NMDA EPSCs were more reduced in the absence than the presence of Mg^{2+} (−40 mV, $p < 0.0001$; +40 mV; $p < 0.001$). Thus, the extent of influence of Mg^{2+} on CP-101,606 sensitivity may depend on the presence of different NR2B-containing NMDARs at P5 versus P28.

To investigate the influence of Mg^{2+} on the sensitivity of CP-101,606 independent of NR1/NR2A/NR2B receptors, we examined the effect of CP-101,606 on NMDA EPSCs in CA1 cells of adult *NR2A*$^{-/-}$ mice, which contain only NR1/NR2B receptors. In the absence of Mg^{2+}, NMDA EPSCs were reduced by about 80% (Fig. 13A), which is comparable to the maximal antagonism of recombinant NR1/NR2B receptors (80-90%; Mott et al., 1998; Williams, 1993). In the presence of Mg^{2+}, the effect of CP-101,606 was significantly reduced (−40 mV, $p < 0.001$; +40 mV, $p < 0.01$; Fig. 13B), indicating that the sensitivity of CP-101,606 is enhanced in the absence of Mg^{2+}. As the reduction of the CP-effect by Mg^{2+} is more pronounced for NMDARs in P28 wild-type than for NR1/NR2B receptors in *NR2A*$^{-/-}$ mice (Fig. 11 vs. Fig. 13), the absence of Mg^{2+} seems to strengthen the antagonism by CP-101,606 even more for triheteromeric NMDARs. Thus, antagonism is reduced by presence of NR2A (Brimecombe et al., 1997; Hatton and Paoletti, 2005; Tovar and Westbrook, 1999) and also by the presence of Mg^{2+}, as shown in Figs. 11 and 12.

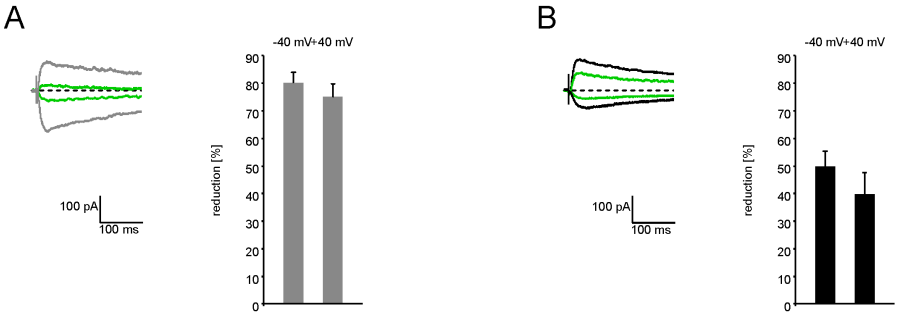

Fig. 13: Effects of CP-101,606 on NMDA EPSCs in adult *NR2A*$^{-/-}$ mice. Averaged representative current traces show NMDA EPSCs at −40 and +40 mV in absence (**A**, grey) and presence (**B**, black) of Mg^{2+} before and after (green) perfusion of CP-101,606 (10 μM). **A**, In Mg^{2+}-free Ringer solution, CP-101,606 reduced NMDA EPSCs at −40 mV by 80.33 ± 3.83% (n = 7) and +40 mV by 75.13 ± 4.53% (n = 7). **B**, In the presence of 1 mM Mg^{2+}, reduction of NMDA EPSCs by CP-101,606 was reduced compared to Mg^{2+}-free conditions (−40 mV, $p < 0.001$; +40 mV, $p < 0.01$; reduction at −40 mV, 49.90 ± 5.41%, n = 7; +40 mV, 39.71 ± 7.86%, n = 7).

3 Discussion

Key to this study was the analysis of the voltage dependence of NMDA EPSC decay time in combination with the use of NR2B-directed NMDAR antagonists in acute hippocampal slices of wild-type and two lines of gene-targeted mice, *NR2A*$^{-/-}$ and *NR2B*$^{\Delta Fb}$ mice. The disruption of the NR2A subunit in *NR2A*$^{-/-}$ is reported to have no effect on the mRNA expression of the remaining NMDAR subunits. In addition, in *NR2B*$^{\Delta Fb}$ mice, no compensatory increase in NR2A expression was observed, suggesting that no compensation of NMDAR subunit expression occurred in the two gene-targeted mouse lines (Sakimura et al., 1995; von Engelhardt et al., 2008). Our results ascertain the presence of NR2B-containing NMDARs in CA3-to-CA1 synapses throughout development and identify triheteromeric NR1/NR2A/NR2B receptors as a prominent NMDAR population (>50%) in CA1 synapses of adult wild-type mice (P28/P44).

3.1 NMDA receptor composition of hippocampal synapses

Triheteromeric NMDARs form without doubt (Al-Hallaq et al., 2007; Brickley et al., 2003; Chazot et al., 1994; Kew et al., 1998; Luo et al., 1997; Sheng et al., 1994; Tovar and Westbrook, 1999), but testing their relative abundance is delicate. Biochemical approaches analyzing membrane fractions yielded different amounts of triheteromeric NMDARs even within the same brain structure (Al-Hallaq et al., 2007; Chazot et al., 1994; Kew et al., 1998; Luo et al., 1997; Sheng et al., 1994). To identify different NMDAR subtypes within distinct circuits, e.g. at CA3-to-CA1 synapses, electrophysiologists usually test the sensitivity of NMDA EPSCs to NMDAR antagonists, which were primarily characterized for recombinant diheteromeric NMDARs. This approach allows conclusions regarding NR2B-containing (NR2B-type) NMDARs but does not permit a rigorous distinction between di- and triheteromeric NMDARs. During the first

postnatal week, NMDA EPSCs in CA1 neurons are highly sensitive to NR2B-directed NMDAR antagonists (our study; Bellone and Nicoll, 2007; Brothwell et al., 2008; de Marchena et al., 2008; Lopez de Armentia and Sah, 2003). Here, in adult wild-type mice (P28/P44), CP-101,606 reduced NMDA EPSCs about 50% in the absence of Mg^{2+}. Consistently, in mice older than five weeks, ifenprodil reduced NMDA EPSCs by around 40% (Kirson and Yaari, 1996). Thus, experiments with two different NR2B-specific antagonists support the hypothesis that NR2B-containing NMDARs remain present in hippocampal synapses throughout development. This is consistent with immunogold labeling of postsynaptic densities (Köhr et al., 2003) and with our analysis of the NMDA EPSC decay time in the three genotypes, showing that the decay time of NMDA EPSCs in adult wild-type mice was 2-fold slower than the respective decay time for NR1/NR2A receptors in $NR2B^{\Delta Fb}$ mice. However, synaptic NR1/NR2B receptors deactivate 6-9-fold slower than synaptic NR1/NR2A receptors. This argues against a 50% contribution of NR1/NR2B receptors to NMDA EPSCs in wild type, because the NMDA EPSC decay time is not halfway of that of the diheteromeric NMDARs. Indeed, our demonstration that the voltage dependence of NMDA EPSC decay is distinct for NR1/NR2B and NR1/NR2A receptors argues for a definite presence of NR1/NR2A/NR2B receptors in adult synapses. If NR1/NR2B receptors were to predominate in adult wild-type hippocampal synapses, their distinct voltage dependence of decay would have caused a higher $-40/+40$ mV ratio of decay time constants than the one we observed. In fact, the voltage dependence of decay is identical in adult wild-type and $NR2B^{\Delta Fb}$ mice. Consequently, the NR2B-containing receptors in adult wild-type mice represent mainly NR1/NR2A/NR2B receptors. These synaptic triheteromeric NR1/NR2A/NR2B receptors mediate NMDA EPSCs with slower deactivation kinetics than diheteromeric NR1/NR2A receptors but display the NR1/NR2A-like voltage dependence of decay. Therefore, in NR1/NR2A/NR2B receptors, the presence of NR2B likely slows the deactivation but the presence of NR2A confers the voltage dependence of decay. This combination indicates a new property of NMDARs that cannot be explained by a mixture of diheteromeric NR1/NR2A and NR1/NR2B receptors.

Outside synapses, NR1/NR2B receptors may exist and explain the finding of a recent quantitative biochemical study, showing that NR1/NR2A, NR1/NR2B

and NR1/NR2A/NR2B receptors each constitute approximately one-third of the total NMDAR population at P7, P42, and 6 months (Al-Hallaq et al., 2007). On the other hand, constant proportions of the three NMDAR subtypes throughout development in the whole hippocampus are not in agreement with the increasing NR2A/NR2B ratio during development (Monyer et al., 1994; Watanabe et al., 1993). Indeed, the change in the synaptic NMDAR content during development due to increased NR2A contribution is indicated by two facts: (1) the decay time constant of NMDA EPSCs decreases during development, as seen in this and previous studies, and (2) the sensitivity to NR2B-directed NMDAR antagonists usually decreases (for review, see e.g. Köhr, 2006; but also section 3.3).

In neonatal wild-type mice, the presence of synaptic NR1/NR2B receptors was suggested by the slowdown of NMDA EPSCs during Mg^{2+} washout exclusively at negative potentials, although synaptic NR1/NR2B receptors failed to show the distinct voltage dependence of NMDA EPSC decay time observed in adult *NR2A*$^{-/-}$ mice. Therefore, in neonatal wild-type mice, we could not distinguish whether CP-101,606 antagonized NR1/NR2B, NR1/NR2A/NR2B and/or other NR2B-containing triheteromeric NMDARs, which may include NR2D or NR3 subunits, although their presence in CA1 pyramidal cells is still unclear (for review, see Stephenson et al., 2008). In any case, these latter subunit combinations and/or additional factors regulating NR1/NR2B receptor-mediated NMDA EPSC decay time in neonatal wild-type mice implicate that NMDA EPSC decay time ratios are constant over development, since NR1/NR2B receptors are a minor population in adult synapses.

The existence of triheteromeric NMDARs in adult mice raises the question as to their function. Since it is impossible to examine this NMDAR population in isolation, the role of NR1/NR2A/NR2B receptors remains speculative. Presence of NR2B within synaptic NMDARs could be essential at all developmental stages, as NR2B, compared to NR2A, allows binding with higher affinity to molecules important for NMDAR signaling or internalization, e.g. CaMKII (Barria and Malinow, 2005; Bayer et al., 2001), rasGRF1 (Kim et al., 2005; Krapivinsky et al., 2003) or the clathrin adaptor protein AP-2 (Roche et al., 2001). Regarding synaptic plasticity in hippocampal synapses, magnitude of NMDAR-dependent LTP and charge transfer during induction by low frequency stimulation correlate

(Berberich et al., 2007). Presence of NR2B in *NR2A*$^{-/-}$ mice preserves LTP (Kiyama et al., 1998), but LTP is impaired in NR2B-lacking CA1 neurons of *NR2B*$^{\Delta Fb}$ mice (von Engelhardt et al., 2008). Thus, we propose that presence of NR2B within NR1/NR2A/NR2B receptors in adult wild-type mice is crucial for charge transfer during hippocampal LTP induction, learning, and memory.

3.2 Evidence for triheteromeric NMDA receptors at different synapses in the CNS

Our study identifies triheteromeric NR1/NR2A/NR2B receptors to represent a prominent NMDAR population in adult hippocampal synapses. We characterized this major population by the new combination of voltage dependence of decay and decay time. This observation suggests that also other triheteromeric NMDARs could have unique receptor properties and thus expand the diversity of NMDAR function.

In heterologous expression systems, coexpression of different NR2 subunits with the NR1 subunit resulted in formation of triheteromeric NMDARs. Examining the concentration-response curves to glycine in Xenopus oocytes coexpressing NR1, NR2A, and NR2C revealed that a triheteromeric receptor containing all of these subunits is preferentially formed (Wafford et al., 1993). In Chinese hamster ovary cells transfected with NR1, NR2A, and NR2B, single-channel recordings on outside-out patches exposed a small number of cells with properties intermediate to NR1/NR2A and NR1/NR2B, including insensitivity to CP-101,606 but redox properties similar to NR1/NR2B. This was interpreted to be consistent with the coassembly of NR2A with NR2B (Brimecombe et al., 1997). In addition to triheteromeric NR1/NR2 receptors, the NR3 subunit has been shown in heterologous expression systems to assemble in a triheteromeric complex of NR1, NR2, and NR3 to form an NMDAR with novel properties and attenuated currents compared to NR1/NR2 NMDARs (for review, see Henson et al., 2010).

Using various approaches, different subtypes of triheteromeric NMDARs combining different NR2 subunits have been described in several brain regions in addition to CA3-to-CA1 synapses. The investigation of somatic NMDARs in new-

born rat hippocampal granule cells by single-channel recordings of outside-out patches suggested that NMDARs in P0 hippocampal granule cells are a mixture of NR1/NR2B and triheteromeric NR1/NR2B/NR2D receptors. This was concluded from the consideration of the biophysical properties of the channel, namely the pattern of single-channel activity, and the sensitivity to ifenprodil (Piña-Crespo and Gibb, 2002).

NR1/NR2B/NR2D as well as NR1/NR2A/NR2D have been discovered by immunoprecipitation in rat thalamus, cortex, and midbrain (Dunah et al., 1998). Accordingly, NR1/NR2B/NR2D receptors have been described to exist in rat substantia nigra dopaminergic neurons. A combination of single-channel recordings and pharmacological approaches was used to identify somatic NR1/NR2B/NR2D receptors (Jones and Gibb, 2005), and these receptors have also been shown to form a significant fraction of synaptic NMDARs (Brothwell et al., 2008). In the latter study, electrophysiological recordings were performed in acute midbrain-containing slices and the effect of different pharmacological drugs on NMDA EPSCs was used to conclude for the subtypes present in synapses. However, the decrease of NMDA EPSC time constants over development as well as the developmental profile of NR2D mRNA expression did not support the concluded synaptic NMDAR composition.

Furthermore, the comparison of NMDAR channel activity in cerebellar Golgi cells in acute cerebellar slices from wild-type and *NR2D*$^{-/-}$ mice (P7-P10) suggests that triheteromeric NR1/NR2B/NR2D receptors are present in Golgi cells of wild type, but that this receptor subtype is restricted to extrasynaptic sites (Brickley et al., 2003). In contrast, Didier et al. (1995) reported that only low levels of NR2D mRNA can be detected by *in situ* hybridization in cerebellar nuclei, the Purkinje layer, and the molecular layer over development. They performed additional immunoprecipitation experiments and consequently proposed that, at early stages, the predominant NMDAR subtype includes NR1, NR2A, and NR2B in the same complex. However, another study described the existence of NMDARs in the adult mouse cerebellum with a pharmacological profile similar to that displayed by the coexpression of NR1/NR2A/NR2C subunits in human embryonic kidney 293 cells (Chazot et al., 1994).

In contrast to the divergent results concerning triheteromeric NMDARs in the

cerebellum, triheteromeric NR1/NR2A/NR2B in the cortex have consistently been reported by both biochemical and electrophysiological studies, but their proportion of the total NMDAR population is still unclear (Kew et al., 1998; Luo et al., 1997; Sheng et al., 1994).

In a recent study, it was postulated that the mature NMDAR subtype at the calyx-of-Held-medial nucleus of the trapezoid body synapse is a triheteromeric NR1/NR2A/NR2C receptor (Steinert et al., 2010). The conclusion that the NMDAR population at this synapse consists rather of a single triheteromeric receptor subtype than of two independent diheteromeric NMDAR populations is based on the observation that the slow and the fast component of the decay time constant describing the biphasic decay kinetics showed similar pharmacology and age-dependent changes. However, outside-out patches from cells expressing exclusively recombinant NR1/NR2A receptors decay in a biphasic manner and the fast and the slow components have been shown to arise from the simultaneous deactivation of receptors that gate with short and long openings, respectively (Zhang et al., 2008). Thus, effects on the two components of the decay time constant might not necessarily be related to the NMDAR population present in a synapse.

In summary, triheteromeric NMDARs including two NR1 and two different NR2 or NR3 subunits with properties distinct from diheteromeric NMDARs contribute to synaptic transmission at different synapses in the CNS.

3.3 NR2B-directed antagonists and related issues

The postnatal appearance of NR2A in many brain areas is often correlated to a decrease in the sensitivity of NMDA EPSCs to NR2B-directed antagonists (for review, see e.g. Köhr, 2006). We also observed a developmental decrease in the antagonist sensitivity of ifenprodil and CP-101,606 in wild-type mice as long as we recorded NMDA EPSCs in the presence of Mg^{2+}. This was not observed in the absence of Mg^{2+} and suggested that recording conditions influence the sensitivity of both NR2B-directed NMDAR antagonists in slices. We confirmed this possibility for CP-101,606 in adult *NR2A*$^{-/-}$ mice, which lack NR1/NR2A and NR1/NR2A/NR2B receptors, by showing that NMDA EPSCs were antagonized stronger in absence than in presence of Mg^{2+}. This influence of Mg^{2+} appears to be

restricted to acute slices, since ifenprodil antagonized recombinant NR1/NR2B receptors to similar extents in absence and in presence of Mg^{2+} (Hatton and Paoletti, 2005). Consistent with our results in hippocampal slices, in cerebellar slices of P7 rats the extent of NMDA EPSC antagonism by CP-101,606 was never as strong as that observed for recombinant NR1/NR2B receptors ($\leq$70%, Rumbaugh and Vicini, 1999). Yet, the 80% reduction of NR1/NR2B receptor-mediated NMDA EPSCs by CP-101,606 observed under Mg^{2+}-free conditions ($\leq$4.5 μM) is close to the maximal (80-90%) reduction of agonist evoked currents mediated by recombinant NR1/NR2B receptors (Mott et al., 1998; Williams, 1993). Thus, to achieve maximal antagonism by NR2B-directed NMDAR antagonists in slices, absence of Mg^{2+} is recommended. This is particularly important when triheteromeric NMDARs are present because in the presence of Mg^{2+} antagonism by CP-101,606 of NR1/NR2A/NR2B receptors is more constrained than that of NR1/NR2B receptors. This could be concluded from the observation that the reduction of the CP-effect by Mg^{2+} was more pronounced in wild-type than in *NR2A*$^{-/-}$ mice.

NR2B-directed NMDAR antagonists fail to distinguish between NR1/NR2B and/or NR1/NR2A/NR2B receptors. Both subtypes bind e.g. ifenprodil with high affinity, but currents mediated by both subtypes are reduced to different extents (Hatton and Paoletti, 2005). The ifenprodil derivatives CP-101,606 and Ro25-6981, which have significantly higher affinity for NR1/NR2B receptors than ifenprodil (Chazot et al., 2002; Fischer et al., 1997; Williams, 1993), were previously proposed to represent two classes of NR2B-directed NMDAR antagonists (Chazot et al., 2002). Ro 25,6981 was found to bind with comparable high affinities to both NR1/NR2B and NR1/NR2A/NR2B receptors (Hawkins et al., 1999), whereas binding of CP-101,606 was significantly reduced by the presence of another NR2 subunit within the NMDAR complex (Chazot et al., 2002). Unfortunately, this distinction did not apply when examining the decrease of NMDA EPSCs by CP-101,606 in wild-type mice. The 50% reduction of NMDA EPSCs by CP-101,606 in the absence of Mg^{2+} in P28 wild-type mice demonstrates that CP-101,606 blocks NR1/NR2A/NR2B receptors besides NR1/NR2B receptors. Therefore, ifenprodil and its derivatives are NR2B-directed, but not NR1/NR2B-selective antagonists. Furthermore, the 50% reduction of NMDA EPSCs by CP-101,606 identifies triheteromeric NMDARs as the foremost NMDAR subtype (>50%) in adult synapses,

since maximal antagonism of NR1/NR2B receptors is 80-90% (Mott et al., 1998; Williams, 1993), and the extent of antagonism is reduced for NR1/NR2A/NR2B receptors (Hatton and Paoletti, 2005).

In wild type, inhibition of the slow decaying NR1/NR2B receptors by NR2B-directed antagonists is expected to accelerate the NMDA EPSC deactivation. As NR2B-directed antagonists have been reported to act in a voltage-independent manner (Mott et al., 1998; Williams, 1993), the effect on NMDA EPSC deactivation is anticipated to be similar at negative and positive membrane potentials. However, we observed in our experiments that CP-101,606 accelerated the deactivation exclusively at +40 mV and not at −40 mV, although NMDA EPSC amplitudes were similarly reduced at both membrane potentials (see also Punnakkal et al., 2006). Usually, effects of NR2B-directed antagonists on NMDA EPSC decay are investigated exclusively at negative or at positive membrane potentials. Accordingly, ifenprodil has been described to accelerate the NMDA EPSC decay at +40 mV (Bellone and Nicoll, 2007; de Marchena et al., 2008), but the NMDA EPSC decay at −40 mV has not been altered by ifenprodil (Kirson and Yaari, 1996) or CP-101,606 (Longordo et al., 2009).

The CA3-to-CA1 synapse is well established for the investigation of molecular processes underlying learning and memory, and the role of NMDARs in physiological and pathological conditions has been widely studied. Nevertheless, the actual subunit composition of these receptors in the hippocampal circuit has been not ascertained yet. The study presented here offers a better understanding of NMDARs at this synapse by identifying triheteromeric receptors as being the major players in mature CA3-to-CA1 connections. Our findings extend the understanding of NMDAR function during physiological synaptic transmission and have to be considered for the design of new pharmacological strategies to precisely target a specific subtype in order to counteract the deleterious effects of pathological NMDAR function.

4 Materials and Methods

4.1 Mouse genotyping

The tips of mouse tails were digested by proteinase K (1 mg/ml) in TENS buffer (50 mM Tris-HCl pH 8.0, 100 mM EDTA, 100 mM NaCl, 1% SDS) at 55°C. After precipitation in one volume of isopropanol and washing with 70% ethanol, genomic DNA was diluted by shaking for 30 min in 300 μl of sterile H_2O (Millipore) at 55°C. For PCR analysis, 1 μl of this solution was used to perform the PCR reaction as detailed below.

PCR-protocol for genotyping *NR2A*$^{-/-}$ mice

PCR-mix for 10 PCR reactions:

PCR-buffer	[10 x]	25 μl
$MgCl_2$	[50 mM]	10 μl
dNTPs	[20 mM]	10 μl
primer PGK Prom2	[10 μM]	5 μl
primer 2AIN10N*do	[10 μM]	5 μl
primer 2AIN11x*up	[10 μM]	10 μl
H_2O		174 μl
Taq Polymerase		1 μl

PGK Prom2: 5'-CAGACTGCCTTGGGAAAAGCG-3'
2AIN10N*do: 5'-GGGAATTCGCGGCCGCAAGAGCAAGAAGACTCC-3'
2AIN11x*up: 5'-GGAGGTACCTCGAGCTCTTCTACAG-3'

PCR: 24 μl PCR-mix + 1 μl DNA-Preparation
PCR-protocol:

Temp.	Time	
96°C	3 min	
96°C	20 s	
55°C	30 s	35 cycles
72°C	75 s	
72°C	10 min	

Expected Bands:

NR2A WT: about 580 bp

NR2A$^{-/-}$: about 1100 bp

PCR-protocol for genotyping *NR2B*$^{\Delta Fb}$ mice

PCR-mix for 10 PCR reactions:

PCR-buffer	[10 x]	62.5 μl
$MgCl_2$	[50 mM]	25 μl
dNTPs	[20 mM]	25 μl
2 B 3'	[10 μM]	12.5 μl
2 B 5'	[10 μM]	12.5 μl
H_2O		460 μl
Taq Polymerase		2.5 μl

2 B 3': 5'-GAGTTGCCTCCATCATTGTGTC-3'
2 B 5': 5'-AGTCTCCTCTTCATCCTCAGTG-3'

PCR: 24 μl PCR-mix + 1 μl DNA-Preparation
PCR-protocol:

Temp.	Time	
95°C	1 min	
95°C	15 s	
55°C	20 s	35 cycles
72°C	30 s	
72°C	5 min	

Expected Bands:
NR2B WT: about 213 bp
NR2B$^{\Delta Fb}$: about 329 bp

All animals were re-genotyped following experiments.

4.2 Slice preparation

All experimental procedures were in accordance with the animal welfare guidelines of the Max Planck Society. Deeply anesthetized (isoflurane; Baxter, Germany) wild-type (WT, C57Bl/6), *NR2A*$^{-/-}$ (Sakimura et al., 1995), and *NR2B*$^{\Delta Fb}$ mice (von Engelhardt et al., 2008) (P5, P4-P6; P28, P27-P29 or P44, P41-P48) were decapitated and their brains were removed. For neonatal (P5) mice, coronal hippocampal slices (250 μm) were prepared using artificial cerebrospinal fluid (ACSF) containing (in mM): 125 NaCl, 25 $NaHCO_3$, 2.5 KCl, 1.25 NaH_2PO_4, 1 $MgCl_2$, 25 glucose, 2 $CaCl_2$ (Biometra, Göttingen, Germany); bubbled with 95% O_2/5% CO_2 (pH 7.3, 320 mOsm). The cerebellum, olfactory bulb, and part of the prefrontal cortex were removed with a razor blade. The brain was glued (cyanoacrylate glue; UHU, Germany) with the cut surface of the prefrontal cortex onto a metal plate, which was then tightly fixed in a slicing chamber. For adult (P28/P44) mice, transverse hippocampal slices were prepared using either a modified ACSF containing (in mM): 125 NaCl, 25 $NaHCO_3$, 2.5 KCl, 1.25 NaH_2PO_4, 6 $MgCl_2$, 25 glucose, 1 $CaCl_2$, 3 myo-Inositol, 2 Na-pyruvat, 0.4 vitamin C, or a slicing solution containing (in mM): 140 K-gluconate, 10 HEPES, 15 Na-gluconate, 0.2 EGTA, 4 NaCl (pH 7.2); both bubbled with 95% O_2/5% CO_2. First, the cerebellum was removed with a razor blade, then, the hemispheres were separated along the mid-

line. One hemisphere was placed on the cut surface and 1-2 mm of the apical cortex was removed by a cut perpendicular to the midline. The hemisphere was glued (cyanoacrylate glue; UHU, Germany) with the cut surface facing down onto a metal plate, which was then tightly fixed in a slicing chamber. The slices were prepared at 4°C using a vibratome (Sigmann Elektronik, Hüffenhardt, Germany) with a razor blade at an angle of 12° to horizontal. Slices were transferred to a recovery chamber filled with oxygenated ACSF, recovered for one hour at 35°C and were maintained at room temperature (22-25°C) up to 8 hours after slicing.

4.3 Electrophysiology

4.3.1 Patch-clamp technique

The patch-clamp technique developed by Neher and Sakmann and originally used for single-channel current recordings allows the recording of the electrical activity of individual neurons (Brenner and Sakmann, 1978; Hamill et al., 1981; Neher and Sakmann, 1976). The main principle is that a tight seal (giga-seal) is formed between a glass pipette and the membrane of a neuron. This so-called cell-attached configuration critically minimizes electrical background noise and therefore allows measuring of small currents and voltages (in the range of picoampere and microvolt) that are involved in neuronal activity. The cell-attached configuration can be converted into different configurations enabling the measurement and control of electrical acitivity. The whole-cell configuration permits recording of either transmembrane currents if the voltage is kept constant (voltage-clamp mode) or of changes in the membrane potential resulting from current flow via ion channels if a constant current is applied (current-clamp mode).

Briefly, the patch-clamp amplifier is set to voltage-clamp mode and a command voltage pulse of -5 mV and 10 ms duration is applied to the electrode. Positive pressure is applied to the pipette to keep the tip clean when entering the bath solution and the slice. The resistance of the pipette can be calculated by Ohm's law using the amplitude of the current response to the -5 mV voltage step. Under visual control, the pipette tip is targeted through the slice to the soma of a visually identified neuron. The pipette tip is slowly brought close to the soma until a

small dimple on the cell membrane becomes visible. Then, the positive pressure is released and slight suction is applied. The membrane starts to seal onto the pipette tip, which can be monitored in the electrical current recording: the current from the pipette tip decreases rapidly because of the formation of a tight seal between the pipette tip and the cell membrane. When almost no measurable current is flowing, the giga-seal with a resistance between the pipette and the bath solution in the order of GΩ is established. Capacitive currents arising by the applied voltage step to the cell membrane are compensated. The voltage command is set to −70 mV and after the establishment of the giga-seal, the membrane below the pipette tip is disrupted by applying a transient suction pulse. The contact between the electrode and the cytoplasm of the cell determines the series resistance (R_s), whereas the passive electrical properties of the cell determine the input resistance (R_i).

4.3.2 Patch-clamp setup

Electrophysiological recordings from CA1 hippocampal neurons were performed with the patch-clamp amplifier EPC-9 (HEKA, Lambrecht, Germany) operating in voltage-clamp mode.

Acute hippocampal slices were placed in a recording chamber constantly perfused with oxygenated ACSF and fixed by a grid made of a platinum frame spanned with dental floss. Hippocampal CA1 pyramidal neurons were visualized using an upright fixed-stage microscope (Axioskop 1; Zeiss, Göttingen, Germany) equipped with a 5x objective (Plan-NEOFLUAR; Zeiss), a 60x water immersion objective (LUMPlanFl; Olympus, Tokyo, Japan) and an infrared-sensitive video camera (C2400; Hamamatsu, Japan) combined with a 1.6x magnification. The preamplifier headstage holding the patch pipette and the stimulation pipette holder were mounted on motorized micromanipulators (Mini 25; Luigs&Neumann, Ratingen, Germany). Extracellular stimulation in stratum radiatum was performed with a stimulus isolator (WPI, Saratosa, USA). Patch and stimulation pipettes were pulled from thick-walled (0.5 mm) borosilicate glass capillaries (Hilgenfeld, Malsfeld, Germany) on a horizontal pipette puller (P-97; Sutter Instruments, Novato, CA, USA). The micromanipulators together with the recording chamber were

mounted on a motorized xy-translation table to allow movement of the sample and the pipettes below the fixed optical axis of the microscope. The extracellular solution was grounded with an Ag/AgCl pellet via the reference input of the preamplifier headstage. The solution in the pipettes was in electrical contact with the preamplifier via a chlorinated silver wire.

The optical and mechanical instruments were mounted to a vibration-isolation table (Physik Instrumente, Karlsruhe, Germany) to minimize vibrations and were surrounded by a Faraday cage in order to minimize electrical noise during the recordings.

4.3.3 Synaptic current recordings

Single slices were transferred from the recovery chamber to the recording chamber and continuously perfused with oxygenated ACSF containing 10 μM Bicuculline methiodide or 5 μM Gabazine, 10 μM NBQX and 10 μM glycine. CA1 pyramidal neurons were identified due to their characteristic morphology by using infrared differential interference contrast microscopy. Patch pipettes had resistances of 3.5-6.5 MΩ when filled with (in mM): 125 Cs-gluconate, 20 CsCl, 10 NaCl, 10 HEPES, 0.2 EGTA, 4 MgATP, 0.3 Na_3GTP, 2.5 QX-314Cl^- (pH 7.3, 270-320 mOsm). Liquid junction potential was not corrected. Series and input resistances were continuously monitored by measuring peak and steady-state currents in response to hyperpolarizing pulses (-5 mV, 20 ms), and cells were excluded if series resistance changed by more than 20%.

Pharmacologically isolated NMDA EPSCs were evoked in CA1 pyramidal cells by electrical stimulation of Schaffer collaterals at 0.1 Hz in stratum radiatum about 150 μm distant from the CA1 cell body layer with monopolar glass pipettes filled with 1 M NaCl. NMDA EPSCs were recorded at -40 and $+40$ mV in the presence of 1 mM Mg^{2+} (ACSF) or following 25 minutes of Mg^{2+} washout using nominally Mg^{2+}-free ACSF (in mM): 125 NaCl, 25 $NaHCO_3$, 2.5 KCl, 1.25 NaH_2PO_4, 25 glucose, 2 $CaCl_2$ (pH 7.3, 310 mOsm). During Mg^{2+} washout, electrical stimulation was preserved at 0.1 Hz. The Mg^{2+} concentration was 1.5 μM in freshly prepared Mg^{2+}-free ACSF and $\leq$4.5 μM in ACSF collected following 25 minutes of slice perfusion (ICP-optical emission spectrometry by Christian Scholz, University of

Heidelberg). In the absence of Mg^{2+}, I-V curves were linear between −40 mV and +40 mV, and raising the temperature from room temperature (22-25°C) to near physiological temperature (31-33°C) had no effect on both reversal potential and peak amplitudes (Fig. 14). Consequently, experiments were performed at room temperature. In some experiments, the NMDAR antagonist D-APV (Biotrend) or one of the two NR2B-directed antagonists CP-101,606 (Pfizer) or ifenprodil (Sigma) were present. NR2B-directed NMDAR antagonists were washed in for 20 minutes either in the presence or absence of Mg^{2+} before their effects on NMDA EPSCs were determined.

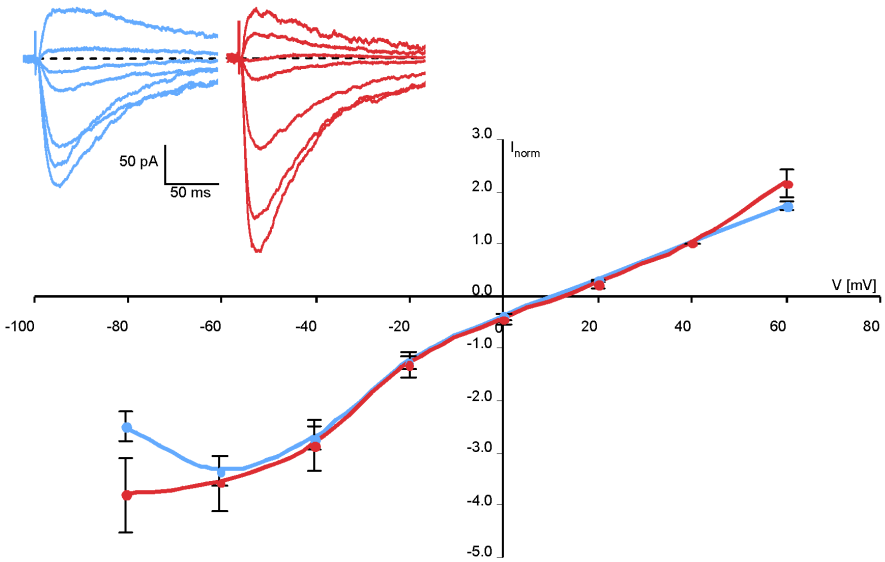

Fig. 14: I-V curves recorded in the absence of Mg^{2+} at room temperature and at near-physiological temperature. I-V curves were recorded at room temperature (blue) and near-physiological temperature (red) in 20 mV steps from -80 mV to +60 mV and normalized to the respective peak amplitude at +40 mV. Peak amplitudes at all membrane potentials were not different at room temperature (n = 17) and at near physiological temperature (n = 9, $p > 0.05$ for all membrane potentials). Inset shows representative I-V curves from −80 mV to +40 mV in 20 mV steps at room temperature (left, blue) and near-physiological temperature (right, red) recorded in the same cell.

4.3.4 Data acquisition and analysis

Synaptic responses were filtered at 3 kHz and digitized at 10 kHz using the AD-converter of the EPC-9 (ITC-16; Instrutech, Great Neck, NY, USA). The amplifier and the ITC-16 were controlled by Pulse/Patchmaster software (HEKA, Lambrecht, Germany) on a Macintosh Power PC (Apple, Cupertino, CA, USA). Visually identified polysynaptic NMDA EPSCs were excluded and monosynaptic currents were averaged over 1.5 minutes of recording. The programs Pulsefit/Fitmaster were used for off-line analysis of peak amplitudes and decay time. Averaged NMDA EPSCs were fitted biexponentially (Zhang et al., 2008), and weighted Taus (ms) were calculated using following formula:
$\mathrm{Tau}_{weighted} = (\mathrm{I}_{fast}/(\mathrm{I}_{fast}+\mathrm{I}_{slow}))*\mathrm{Tau}_{fast} + (\mathrm{I}_{slow}/(\mathrm{I}_{slow}+\mathrm{I}_{fast}))*\mathrm{Tau}_{slow}$, where I is the amplitude of the fast or slow component, and Tau is the respective decay time constant (Stocca and Vicini, 1998). For each cell, at least two $\mathrm{Tau}_{weighted}$ were averaged for each recording condition, before the voltage dependence of decay was estimated by the ratio $\mathrm{Tau}_{weighted}$ at -40 mV divided by $\mathrm{Tau}_{weighted}$ at $+40$ mV. Data are presented as mean $\pm$ SEM. Statistical significance was evaluated by paired ($^{\#,\dagger}$) or unpaired (*) Student's t-tests, and ANOVA with Fisher's LSD post-hoc analysis. $p < 0.05$ was regarded as significant.

5 Abbreviations

ACSF	artificial cerebrospinal fluid
AMPA	L-α-amino-3-hydroxy-5-methyl-4-isoxazolepropionic acid
AMPAR	AMPA receptor
BMI	bicuculline methiodide
C	Celsius
CA	cornu ammonis
Ca^{2+}	calcium
CaMKII	Ca^{2+}/calmodulin-dependent protein kinase II
Cl^{-}	chloride
CNS	central nervous system
CTD	carboxy-terminal domain
D-AP5	(D)-2-amino-5-phosphonopentanoate
DG	dentate gyrus
EDTA	ethylene diaminetetraacetic acid
GABA	γ-aminobutyric acid
EC	entorhinal cortex
EPSC	excitatory postsynaptic current
EPSP	excitatory postsynaptic potential
et al.	et alii
e.g.	for example
Fig.	figure
G-protein	guanosine nucleotide-binding protein
GluA-1/2/3/4	AMPA receptor subunit 1/2/3/4
GluK-1/2/3/4/5	Kainate receptor subunit 1/2/3/4/5
GluN1/2/3	NMDA receptor subunit 1/2/3
GluR	glutamate receptor
Hz	Hertz
I	current
i.e.	id est

iGluR	ionotropic glutamate receptor
IPSP	inhibitory postsynaptic potential
K^+	potassium
KA	kainate
LBD	ligand-binding domain
LPP	lateral perforant-path
LTD	long-term depression
LTP	long-term potentiation
μ	micro
m	milli
M	membrane (domain)
M	Mol
m/s	meter/second
Mg^{2+}	magnesium
mGluR	metabotropic glutamate receptor
MPP	medial perforant-path
n	nano
N	asparagine
Na^+	sodium
NBQX	2,3-dihydroxy-6-nitro-7-sulfamoyl-benzo-(F)-quinoxaline
NMDA	N-methyl-D-aspartate
NMDAR	NMDA receptor
NR1	NMDAR subunit 1
NR2A/B/C	NMDAR subunit 2A/B/C
NR3A/B	NMDAR subunit 3A/B
NTD	amino-terminal domain
Ω	Ohm
Osm	Osmol
P	postnatal
PCP	phencyclidine
PSD	postsynaptic density
Q	glutamine
R	arginine

RNA	ribonucleic acid
s	second
S	segment
Sb	subiculum
SEM	standard error of the mean
V	Volts
WT	wild type
Zn^{2+}	zinc

6 Bibliography

Al-Hallaq RA, Conrads TP, Veenstra TD & Wenthold RJ (2007). NMDA di-heteromeric receptor populations and associated proteins in rat hippocampus. *J Neurosci* **27**, 8334–43.

Amato A, Ballerini L & Attwell D (1994). Intracellular pH changes produced by glutamate uptake in rat hippocampal slices. *J Neurophysiol* **72**, 1686–1696.

Araki K, Meguro H, Kushiya E, Takayama C, Inoue Y & Mishina M (1993). Selective expression of the glutamate receptor channel delta 2 subunit in cerebellar Purkinje cells. *Biochem Biophys Res Commun* **197**, 1267–1276.

Auberson YP, Allgeier H, Bischoff S, Lingenhoehl K, Moretti R & Schmutz M (2002). 5-Phosphonomethylquinoxalinediones as competitive NMDA receptor antagonists with a preference for the human 1A/2A, rather than 1A/2B receptor composition. *Bioorg Med Chem Lett* **12**, 1099–102.

Ayalon G & Stern-Bach Y (2001). Functional assembly of AMPA and kainate receptors is mediated by several discrete protein-protein interactions. *Neuron* **31**, 103–113.

Ballard TM, Pauly-Evers M, Higgins GA, Ouagazzal AM, Mutel V, Borroni E, Kemp JA, Bluethmann H & Kew JNC (2002). Severe impairment of NMDA receptor function in mice carrying targeted point mutations in the glycine binding site results in drug-resistant nonhabituating hyperactivity. *J Neurosci* **22**, 6713–6723.

Barria A & Malinow R (2002). Subunit-specific NMDA receptor trafficking to synapses. *Neuron* **35**, 345–53.

Barria A & Malinow R (2005). NMDA receptor subunit composition controls synaptic plasticity by regulating binding to CaMKII. *Neuron* **48**, 289–301.

Barry MF & Ziff EB (2002). Receptor trafficking and the plasticity of excitatory synapses. *Curr Opin Neurobiol* **12**, 279–286.

Barth AL & Malenka RC (2001). NMDAR EPSC kinetics do not regulate the critical period for LTP at thalamocortical synapses. *Nat Neurosci* **4**, 235–6.

Bayer KU, De Koninck P, Leonard AS, Hell JW & Schulman H (2001). Interaction with the NMDA receptor locks CaMKII in an active conformation. *Nature* **411**, 801–5.

Bear MF, Kleinschmidt A, Gu QA & Singer W (1990). Disruption of experience-dependent synaptic modifications in striate cortex by infusion of an NMDA receptor antagonist. *J Neurosci* **10**, 909–925.

Bellone C & Nicoll RA (2007). Rapid Bidirectional Switching of Synaptic NMDA Receptors. *Neuron* **55**, 779–785.

Benveniste M, Clements J, Vyklický L & Mayer ML (1990). A kinetic analysis of the modulation of N-methyl-D-aspartic acid receptors by glycine in mouse cultured hippocampal neurones. *J Physiol* **428**, 333–357.

Benveniste M & Mayer ML (1991). Kinetic analysis of antagonist action at N-methyl-D-aspartic acid receptors. Two binding sites each for glutamate and glycine. *Biophys J* **59**, 560–573.

Benveniste M & Mayer ML (1993). Multiple effects of spermine on N-methyl-D-aspartic acid receptor responses of rat cultured hippocampal neurones. *J Physiol* **464**, 131–163.

Berberich S, Jensen V, Hvalby O, Seeburg PH & Köhr G (2007). The role of NMDAR subtypes and charge transfer during hippocampal LTP induction. *Neuropharmacology* **52**, 77–86.

Berberich S, Punnakkal P, Jensen V, Pawlak V, Seeburg PH, Hvalby O & Köhr G (2005). Lack of NMDA receptor subtype selectivity for hippocampal long-term potentiation. *J Neurosci* **25**, 6907–10.

Bliss TV & Collingridge GL (1993). A synaptic model of memory: long-term potentiation in the hippocampus. *Nature* **361**, 31–9.

Bonifazi P, Goldin M, Picardo MA, Jorquera I, Cattani A, Bianconi G, Represa A, Ben-Ari Y & Cossart R (2009). GABAergic hub neurons orchestrate synchrony in developing hippocampal networks. *Science* **326**, 1419–1424.

Boulter J, Hollmann M, O'Shea-Greenfield A, Hartley M, Deneris E, Maron C & Heinemann S (1990). Molecular cloning and functional expression of glutamate receptor subunit genes. *Science* **249**, 1033–1037.

Brenner HR & Sakmann B (1978). Gating properties of acetycholine receptor in newly formed neuromuscular synapses. *Nature* **271**, 366–368.

Bresink I, Benke TA, Collett VJ, Seal AJ, Parsons CG, Henley JM & Collingridge GL (1996). Effects of memantine on recombinant rat NMDA receptors expressed in HEK 293 cells. *Br J Pharmacol* **119**, 195–204.

Brickley SG, Misra C, Mok MH, Mishina M & Cull-Candy SG (2003). NR2B and NR2D subunits coassemble in cerebellar Golgi cells to form a distinct NMDA receptor subtype restricted to extrasynaptic sites. *J Neurosci* **23**, 4958–66.

Brimecombe JC, Boeckman FA & Aizenman E (1997). Functional consequences of NR2 subunit composition in single recombinant N-methyl-D-aspartate receptors. *Proc Natl Acad Sci U S A* **94**, 11019–24.

Brothwell SL, Barber JL, Monaghan DT, Jane DE, Gibb AJ & Jones S (2008). NR2B- and NR2D-containing synaptic NMDA receptors in developing rat substantia nigra pars compacta dopaminergic neurones. *J Physiol* **586**, 739–50.

Burnashev N (1996). Calcium permeability of glutamate-gated channels in the central nervous system. *Curr Opin Neurobiol* **6**, 311–317.

Burnashev N, Monyer H, Seeburg PH & Sakmann B (1992a). Divalent ion permeability of AMPA receptor channels is dominated by the edited form of a single subunit. *Neuron* **8**, 189–198.

Burnashev N, Schoepfer R, Monyer H, Ruppersberg JP, Gunther W, Seeburg PH & Sakmann B (1992b). Control by asparagine residues of calcium permeability and magnesium blockade in the NMDA receptor. *Science* **257**, 1415–9.

Burnashev N, Zhou Z, Neher E & Sakmann B (1995). Fractional calcium currents through recombinant GluR channels of the NMDA, AMPA and kainate receptor subtypes. *J Physiol* **485**, 403–418.

Buzsáki G & Chrobak JJ (1995). Temporal structure in spatially organized neuronal ensembles: a role for interneuronal networks. *Curr Opin Neurobiol* **5**, 504–510.

Cavara NA & Hollmann M (2008). Shuffling the deck anew: how NR3 tweaks NMDA receptor function. *Mol Neurobiol* **38**, 16–26.

Chaperon F, Müller W, Auberson YP, Tricklebank MD & Neijt HC (2003). Substitution for PCP, disruption of prepulse inhibition and hyperactivity induced by N-methyl-D-aspartate receptor antagonists: preferential involvement of the NR2B rather than NR2A subunit. *Behav Pharmacol* **14**, 477–487.

Chatterton JE, Awobuluyi M, Premkumar LS, Takahashi H, Talantova M, Shin Y, Cui J, Tu S, Sevarino KA, Nakanishi N, Tong G, Lipton SA & Zhang D (2002). Excitatory glycine receptors containing the NR3 family of NMDA receptor subunits. *Nature* **415**, 793–8.

Chazot PL, Coleman SK, Cik M & Stephenson FA (1994). Molecular characterization of N-methyl-D-aspartate receptors expressed in mammalian cells yields evidence for the coexistence of three subunit types within a discrete receptor molecule. *J Biol Chem* **269**, 24403–9.

Chazot PL, Lawrence S & Thompson CL (2002). Studies on the subtype selectivity of CP-101,606: evidence for two classes of NR2B-selective NMDA receptor antagonists. *Neuropharmacology* **42**, 319–24.

Chen N, Moshaver A & Raymond LA (1997). Differential sensitivity of recombinant N-methyl-D-aspartate receptor subtypes to zinc inhibition. *Mol Pharmacol* **51**, 1015–1023.

Chesler M (1990). The regulation and modulation of pH in the nervous system. *Prog Neurobiol* **34**, 401–427.

Chesler M & Kaila K (1992). Modulation of pH by neuronal activity. *Trends Neurosci* **15**, 396–402.

Chizh BA & Headley PM (2005). NMDA antagonists and neuropathic pain–multiple drug targets and multiple uses. *Curr Pharm Des* **11**, 2977–2994.

Christensen JK, Paternain AV, Selak S, Ahring PK & Lerma J (2004). A mosaic of functional kainate receptors in hippocampal interneurons. *J Neurosci* **24**, 8986–8993.

Christine CW & Choi DW (1990). Effect of zinc on NMDA receptor-mediated channel currents in cortical neurons. *J Neurosci* **10**, 108–116.

Ciabarra AM, Sullivan JM, Gahn LG, Pecht G, Heinemann S & Sevarino KA (1995). Cloning and characterization of chi-1: a developmentally regulated member of a novel class of the ionotropic glutamate receptor family. *J Neurosci* **15**, 6498–6508.

Clements JD, Lester RA, Tong G, Jahr CE & Westbrook GL (1992). The time course of glutamate in the synaptic cleft. *Science* **258**, 1498–1501.

Clements JD & Westbrook GL (1991). Activation kinetics reveal the number of glutamate and glycine binding sites on the N-methyl-D-aspartate receptor. *Neuron* **7**, 605–613.

Collingridge GL, Isaac JT & Wang YT (2004). Receptor trafficking and synaptic plasticity. *Nat Rev Neurosci* **5**, 952–62.

Colquhoun D, Large WA & Rang HP (1977). An analysis of the action of a false transmitter at the neuromuscular junction. *J Physiol* **266**, 361–395.

Cull-Candy S, Brickley S & Farrant M (2001). NMDA receptor subunits: diversity, development and disease. *Curr Opin Neurobiol* **11**, 327–35.

Cull-Candy SG & Leszkiewicz DN (2004). Role of distinct NMDA receptor subtypes at central synapses. *Sci STKE* **2004**, re16.

Curtis DR, Phillis JW & Watkins JC (1959). Chemical excitation of spinal neurones. *Nature* **183**, 611–612.

Das S, Sasaki YF, Rothe T, Premkumar LS, Takasu M, Crandall JE, Dikkes P, Conner DA, Rayudu PV, Cheung W, Chen HS, Lipton SA & Nakanishi N (1998). Increased NMDA current and spine density in mice lacking the NMDA receptor subunit NR3A. *Nature* **393**, 377–381.

Davies J, Francis AA, Jones AW & Watkins JC (1981). 2-Amino-5-phosphonovalerate (2APV), a potent and selective antagonist of amino acid-induced and synaptic excitation. *Neurosci Lett* **21**, 77–81.

de Marchena J, Roberts AC, Middlebrooks PG, Valakh V, Yashiro K, Wilfley LR & Philpot BD (2008). NMDA receptor antagonists reveal age-dependent differences in the properties of visual cortical plasticity. *J Neurophysiol* **100**, 1936–48.

Didier M, Xu M, Berman SA & Bursztajn S (1995). Differential expression and co-assembly of NMDA zeta 1 and epsilon subunits in the mouse cerebellum during postnatal development. *Neuroreport* **6**, 2255–2259.

Dingledine R, Borges K, Bowie D & Traynelis SF (1999). The glutamate receptor ion channels. *Pharmacol Rev* **51**, 7–61.

Dudek SM & Bear MF (1992). Homosynaptic long-term depression in area CA1 of hippocampus and effects of N-methyl-D-aspartate receptor blockade. *Proc Natl Acad Sci U S A* **89**, 4363–4367.

Dunah AW, Luo J, Wang YH, Yasuda RP & Wolfe BB (1998). Subunit composition of N-methyl-D-aspartate receptors in the central nervous system that contain the NR2D subunit. *Mol Pharmacol* **53**, 429–437.

Durand GM, Bennett MV & Zukin RS (1993). Splice variants of the N-methyl-D-aspartate receptor NR1 identify domains involved in regulation by polyamines and protein kinase C. *Proc Natl Acad Sci U S A* **90**, 6731–6735.

Fellin T, Pascual O, Gobbo S, Pozzan T, Haydon PG & Carmignoto G (2004). Neuronal synchrony mediated by astrocytic glutamate through activation of extrasynaptic NMDA receptors. *Neuron* **43**, 729–43.

Feng B, Morley RM, Jane DE & Monaghan DT (2005). The effect of competitive antagonist chain length on NMDA receptor subunit selectivity. *Neuropharmacology* **48**, 354–9.

Feng B, Tse HW, Skifter DA, Morley R, Jane DE & Monaghan DT (2004). Structure-activity analysis of a novel NR2C/NR2D-preferring NMDA receptor antagonist: 1-(phenanthrene-2-carbonyl) piperazine-2,3-dicarboxylic acid. *Br J Pharmacol* **141**, 508–16.

Fischer G, Mutel V, Trube G, Malherbe P, Kew JN, Mohacsi E, Heitz MP & Kemp JA (1997). Ro 25-6981, a highly potent and selective blocker of N-methyl-D-aspartate receptors containing the NR2B subunit. Characterization in vitro. *J Pharmacol Exp Ther* **283**, 1285–92.

Fujisawa S & Aoki C (2003). In vivo blockade of N-methyl-D-aspartate receptors induces rapid trafficking of NR2B subunits away from synapses and out of spines and terminals in adult cortex. *Neuroscience* **121**, 51–63.

Fukaya M, Hayashi Y & Watanabe M (2005). NR2 to NR3B subunit switchover of NMDA receptors in early postnatal motoneurons. *Eur J Neurosci* **21**, 1432–1436.

Furukawa H, Singh SK, Mancusso R & Gouaux E (2005). Subunit arrangement and function in NMDA receptors. *Nature* **438**, 185–92.

Gallagher MJ, Huang H, Grant ER & Lynch DR (1997). The NR2B-specific interactions of polyamines and protons with the N-methyl-D-aspartate receptor. *J Biol Chem* **272**, 24971–24979.

Gallagher MJ, Huang H, Pritchett DB & Lynch DR (1996). Interactions between ifenprodil and the NR2B subunit of the N-methyl-D-aspartate receptor. *J Biol Chem* **271**, 9603–9611.

Hamill OP, Marty A, Neher E, Sakmann B & Sigworth FJ (1981). Improved patch-clamp techniques for high-resolution current recording from cells and cell-free membrane patches. *Pflugers Arch* **391**, 85–100.

Hansen KB, Yuan H & Traynelis SF (2007). Structural aspects of AMPA receptor activation, desensitization and deactivation. *Curr Opin Neurobiol* **17**, 281–288.

Hatton CJ & Paoletti P (2005). Modulation of triheteromeric NMDA receptors by N-terminal domain ligands. *Neuron* **46**, 261–74.

Hawkins LM, Chazot PL & Stephenson FA (1999). Biochemical evidence for the co-association of three N-methyl-D-aspartate (NMDA) R2 subunits in recombinant NMDA receptors. *J Biol Chem* **274**, 27211–8.

Haydon PG & Carmignoto G (2006). Astrocyte control of synaptic transmission and neurovascular coupling. *Physiol Rev* **86**, 1009–1031.

Henneberger C, Papouin T, Oliet SHR & Rusakov DA (2010). Long-term potentiation depends on release of D-serine from astrocytes. *Nature* **463**, 232–236.

Henson MA, Roberts AC, Pérez-Otaño I & Philpot BD (2010). Influence of the NR3A subunit on NMDA receptor functions. *Prog Neurobiol* .

Hestrin S (1992). Developmental regulation of NMDA receptor-mediated synaptic currents at a central synapse. *Nature* **357**, 686–9.

Hestrin S, Sah P & Nicoll RA (1990). Mechanisms generating the time course of dual component excitatory synaptic currents recorded in hippocampal slices. *Neuron* **5**, 247–53.

Higuchi M, Single FN, Köhler M, Sommer B, Sprengel R & Seeburg PH (1993). RNA editing of AMPA receptor subunit GluR-B: a base-paired intron-exon structure determines position and efficiency. *Cell* **75**, 1361–1370.

Hollmann M & Heinemann S (1994). Cloned glutamate receptors. *Annu Rev Neurosci* **17**, 31–108.

Hume RI, Dingledine R & Heinemann SF (1991). Identification of a site in glutamate receptor subunits that controls calcium permeability. *Science* **253**, 1028–1031.

Iwasato T, Datwani A, Wolf AM, Nishiyama H, Taguchi Y, Tonegawa S, Knöpfel T, Erzurumlu RS & Itohara S (2000). Cortex-restricted disruption of NMDAR1 impairs neuronal patterns in the barrel cortex. *Nature* **406**, 726–731.

Jahr CE & Stevens CF (1993). Calcium permeability of the N-methyl-D-aspartate receptor channel in hippocampal neurons in culture. *Proc Natl Acad Sci U S A* **90**, 11573–11577.

Janssen WG, Vissavajjhala P, Andrews G, Moran T, Hof PR & Morrison JH (2005). Cellular and synaptic distribution of NR2A and NR2B in macaque monkey and rat hippocampus as visualized with subunit-specific monoclonal antibodies. *Exp Neurol* **191**, 28–44.

Javitt DC (2008). Glycine transport inhibitors and the treatment of schizophrenia. *Biol Psychiatry* **63**, 6–8.

Johnson JW & Ascher P (1987). Glycine potentiates the NMDA response in cultured mouse brain neurons. *Nature* **325**, 529–531.

Johnson JW & Kotermanski SE (2006). Mechanism of action of memantine. *Curr Opin Pharmacol* **6**, 61–7.

Jones S & Gibb AJ (2005). Functional NR2B- and NR2D-containing NMDA receptor channels in rat substantia nigra dopaminergic neurones. *J Physiol* **569**, 209–21.

Kaku DA, Giffard RG & Choi DW (1993). Neuroprotective effects of glutamate antagonists and extracellular acidity. *Science* **260**, 1516–1518.

Kandel E, Schwartz J & Jessell T (2000). *Principles of Neural Science* McGraw-Hill Medical, 4 edition.

Kashiwagi K, Pahk AJ, Masuko T, Igarashi K & Williams K (1997). Block and modulation of N-methyl-D-aspartate receptors by polyamines and protons: role

of amino acid residues in the transmembrane and pore-forming regions of NR1 and NR2 subunits. *Mol Pharmacol* **52**, 701–13.

Kew JN, Richards JG, Mutel V & Kemp JA (1998). Developmental changes in NMDA receptor glycine affinity and ifenprodil sensitivity reveal three distinct populations of NMDA receptors in individual rat cortical neurons. *J Neurosci* **18**, 1935–43.

Kew JN, Trube G & Kemp JA (1996). A novel mechanism of activity-dependent NMDA receptor antagonism describes the effect of ifenprodil in rat cultured cortical neurones. *J Physiol* **497**, 761–72.

Kim KS, Yan D & Tomita S (2010). Assembly and stoichiometry of the AMPA receptor and transmembrane AMPA receptor regulatory protein complex. *J Neurosci* **30**, 1064–1072.

Kim MJ, Dunah AW, Wang YT & Sheng M (2005). Differential roles of NR2A- and NR2B-containing NMDA receptors in Ras-ERK signaling and AMPA receptor trafficking. *Neuron* **46**, 745–60.

Kirson ED & Yaari Y (1996). Synaptic NMDA receptors in developing mouse hippocampal neurones: functional properties and sensitivity to ifenprodil. *J Physiol* **497**, 437–55.

Kiyama Y, Manabe T, Sakimura K, Kawakami F, Mori H & Mishina M (1998). Increased thresholds for long-term potentiation and contextual learning in mice lacking the NMDA-type glutamate receptor epsilon1 subunit. *J Neurosci* **18**, 6704–12.

Kleckner NW & Dingledine R (1988). Requirement for glycine in activation of NMDA-receptors expressed in Xenopus oocytes. *Science* **241**, 835–837.

Köhr G (2006). NMDA receptor function: subunit composition versus spatial distribution. *Cell Tissue Res* **326**, 439–46.

Köhr G, Jensen V, Koester HJ, Mihaljevic AL, Utvik JK, Kvello A, Ottersen OP, Seeburg PH, Sprengel R & Hvalby O (2003). Intracellular domains of

NMDA receptor subtypes are determinants for long-term potentiation induction. *J Neurosci* **23**, 10791–9.

Konnerth A, Keller BU, Ballanyi K & Yaari Y (1990). Voltage sensitivity of NMDA-receptor mediated postsynaptic currents. *Exp Brain Res* **81**, 209–12.

Krapivinsky G, Krapivinsky L, Manasian Y, Ivanov A, Tyzio R, Pellegrino C, Ben-Ari Y, Clapham DE & Medina I (2003). The NMDA receptor is coupled to the ERK pathway by a direct interaction between NR2B and RasGRF1. *Neuron* **40**, 775–84.

Kuner T & Schoepfer R (1996). Multiple structural elements determine subunit specificity of Mg2+ block in NMDA receptor channels. *J Neurosci* **16**, 3549–58.

Kutsuwada T, Sakimura K, Manabe T, Takayama C, Katakura N, Kushiya E, Natsume R, Watanabe M, Inoue Y, Yagi T, Aizawa S, Arakawa M, Takahashi T, Nakamura Y, Mori H & Mishina M (1996). Impairment of suckling response, trigeminal neuronal pattern formation, and hippocampal LTD in NMDA receptor epsilon 2 subunit mutant mice. *Neuron* **16**, 333–44.

Káradóttir R, Hamilton NB, Bakiri Y & Attwell D (2008). Spiking and nonspiking classes of oligodendrocyte precursor glia in CNS white matter. *Nat Neurosci* **11**, 450–456.

Laube B, Kuhse J & Betz H (1998). Evidence for a tetrameric structure of recombinant NMDA receptors. *J Neurosci* **18**, 2954–2961.

Lee JM, Zipfel GJ & Choi DW (1999). The changing landscape of ischaemic brain injury mechanisms. *Nature* **399**, A7–14.

Legendre P, Rosenmund C & Westbrook GL (1993). Inactivation of NMDA channels in cultured hippocampal neurons by intracellular calcium. *J Neurosci* **13**, 674–84.

Legendre P & Westbrook GL (1990). The inhibition of single N-methyl-D-aspartate-activated channels by zinc ions on cultured rat neurones. *J Physiol* **429**, 429–449.

Lerma J (1992). Spermine regulates N-methyl-D-aspartate receptor desensitization. *Neuron* **8**, 343–352.

Lester RA, Clements JD, Westbrook GL & Jahr CE (1990). Channel kinetics determine the time course of NMDA receptor-mediated synaptic currents. *Nature* **346**, 565–7.

Lester RA & Jahr CE (1992). NMDA channel behavior depends on agonist affinity. *J Neurosci* **12**, 635–643.

Li JH, Wang YH, Wolfe BB, Krueger KE, Corsi L, Stocca G & Vicini S (1998). Developmental changes in localization of NMDA receptor subunits in primary cultures of cortical neurons. *Eur J Neurosci* **10**, 1704–15.

Lipton SA (2006). Paradigm shift in neuroprotection by NMDA receptor blockade: memantine and beyond. *Nat Rev Drug Discov* **5**, 160–70.

Liu L, Wong TP, Pozza MF, Lingenhoehl K, Wang Y, Sheng M, Auberson YP & Wang YT (2004). Role of NMDA receptor subtypes in governing the direction of hippocampal synaptic plasticity. *Science* **304**, 1021–4.

Liu Y, Wong TP, Aarts M, Rooyakkers A, Liu L, Lai TW, Wu DC, Lu J, Tymianski M, Craig AM & Wang YT (2007). NMDA receptor subunits have differential roles in mediating excitotoxic neuronal death both in vitro and in vivo. *J Neurosci* **27**, 2846–2857.

Lomeli H, Sprengel R, Laurie DJ, Köhr G, Herb A, Seeburg PH & Wisden W (1993). The rat delta-1 and delta-2 subunits extend the excitatory amino acid receptor family. *FEBS Lett* **315**, 318–322.

Longordo F, Kopp C, Mishina M, Lujan R & Lüthi A (2009). NR2A at CA1 synapses is obligatory for the susceptibility of hippocampal plasticity to sleep loss. *J Neurosci* **29**, 9026–9041.

Lopez de Armentia M & Sah P (2003). Development and subunit composition of synaptic NMDA receptors in the amygdala: NR2B synapses in the adult central amygdala. *J Neurosci* **23**, 6876–83.

Low CM, Zheng F, Lyuboslavsky P & Traynelis SF (2000). Molecular determinants of coordinated proton and zinc inhibition of N-methyl-D-aspartate NR1/NR2A receptors. *Proc Natl Acad Sci U S A* **97**, 11062–7.

Lu W, Shi Y, Jackson AC, Bjorgan K, During MJ, Sprengel R, Seeburg PH & Nicoll RA (2009). Subunit composition of synaptic AMPA receptors revealed by a single-cell genetic approach. *Neuron* **62**, 254–268.

Luo J, Wang Y, Yasuda RP, Dunah AW & Wolfe BB (1997). The majority of N-methyl-D-aspartate receptor complexes in adult rat cerebral cortex contain at least three different subunits (NR1/NR2A/NR2B). *Mol Pharmacol* **51**, 79–86.

Martel MA, Wyllie DJA & Hardingham GE (2009). In developing hippocampal neurons, NR2B-containing N-methyl-D-aspartate receptors (NMDARs) can mediate signaling to neuronal survival and synaptic potentiation, as well as neuronal death. *Neuroscience* **158**, 334–343.

Matsuda K, Fletcher M, Kamiya Y & Yuzaki M (2003). Specific assembly with the NMDA receptor 3B subunit controls surface expression and calcium permeability of NMDA receptors. *J Neurosci* **23**, 10064–10073.

Matsuda K, Kamiya Y, Matsuda S & Yuzaki M (2002). Cloning and characterization of a novel NMDA receptor subunit NR3B: a dominant subunit that reduces calcium permeability. *Brain Res Mol Brain Res* **100**, 43–52.

Mayer ML, Vyklicky L & Clements J (1989a). Regulation of NMDA receptor desensitization in mouse hippocampal neurons by glycine. *Nature* **338**, 425–427.

Mayer ML, Vyklicky L & Westbrook GL (1989b). Modulation of excitatory amino acid receptors by group IIB metal cations in cultured mouse hippocampal neurones. *J Physiol* **415**, 329–350.

Mayer ML & Westbrook GL (1987a). Permeation and block of N-methyl-D-aspartic acid receptor channels by divalent cations in mouse cultured central neurones. *J Physiol* **394**, 501–527.

Mayer ML & Westbrook GL (1987b). The physiology of excitatory amino acids in the vertebrate central nervous system. *Prog Neurobiol* **28**, 197–276.

Mayer ML, Westbrook GL & Guthrie PB (1984). Voltage-dependent block by Mg2+ of NMDA responses in spinal cord neurones. *Nature* **309**, 261–3.

McBain CJ & Mayer ML (1994). N-methyl-D-aspartic acid receptor structure and function. *Physiol Rev* **74**, 723–60.

McGurk JF, Bennett MV & Zukin RS (1990). Polyamines potentiate responses of N-methyl-D-aspartate receptors expressed in xenopus oocytes. *Proc Natl Acad Sci U S A* **87**, 9971–9974.

Meldrum BS (1992). Excitatory amino acid receptors and disease. *Curr Opin Neurol Neurosurg* **5**, 508–513.

Mohn AR, Gainetdinov RR, Caron MG & Koller BH (1999). Mice with reduced NMDA receptor expression display behaviors related to schizophrenia. *Cell* **98**, 427–436.

Monyer H, Burnashev N, Laurie DJ, Sakmann B & Seeburg PH (1994). Developmental and regional expression in the rat brain and functional properties of four NMDA receptors. *Neuron* **12**, 529–40.

Monyer H, Sprengel R, Schoepfer R, Herb A, Higuchi M, Lomeli H, Burnashev N, Sakmann B & Seeburg PH (1992). Heteromeric NMDA receptors: molecular and functional distinction of subtypes. *Science* **256**, 1217–1221.

Mori H, Masaki H, Yamakura T & Mishina M (1992). Identification by mutagenesis of a Mg(2+)-block site of the NMDA receptor channel. *Nature* **358**, 673–675.

Moriyoshi K, Masu M, Ishii T, Shigemoto R, Mizuno N & Nakanishi S (1991). Molecular cloning and characterization of the rat NMDA receptor. *Nature* **354**, 31–37.

Mott DD, Doherty JJ, Zhang S, Washburn MS, Fendley MJ, Lyuboslavsky P, Traynelis SF & Dingledine R (1998). Phenylethanolamines inhibit NMDA receptors by enhancing proton inhibition. *Nat Neurosci* **1**, 659–67.

Mulle C, Sailer A, Swanson GT, Brana C, O'Gorman S, Bettler B & Heinemann SF (2000). Subunit composition of kainate receptors in hippocampal interneurons. *Neuron* **28**, 475–484.

Neher E & Sakmann B (1976). Single-channel currents recorded from membrane of denervated frog muscle fibres. *Nature* **260**, 799–802.

Nicholson KL, Mansbach RS, Menniti FS & Balster RL (2007). The phencyclidine-like discriminative stimulus effects and reinforcing properties of the NR2B-selective N-methyl-D-aspartate antagonist CP-101 606 in rats and rhesus monkeys. *Behav Pharmacol* **18**, 731–743.

Nishi M, Hinds H, Lu HP, Kawata M & Hayashi Y (2001). Motoneuron-specific expression of NR3B, a novel NMDA-type glutamate receptor subunit that works in a dominant-negative manner. *J Neurosci* **21**, RC185.

Nowak L, Bregestovski P, Ascher P, Herbet A & Prochiantz A (1984). Magnesium gates glutamate-activated channels in mouse central neurones. *Nature* **307**, 462–5.

Pan ZZ, Tong G & Jahr CE (1993). A false transmitter at excitatory synapses. *Neuron* **11**, 85–91.

Paoletti P, Ascher P & Neyton J (1997). High-affinity zinc inhibition of NMDA NR1-NR2A receptors. *J Neurosci* **17**, 5711–25.

Paoletti P & Neyton J (2007). NMDA receptor subunits: function and pharmacology. *Curr Opin Pharmacol* **7**, 39–47.

Paulsen O & Moser EI (1998). A model of hippocampal memory encoding and retrieval: GABAergic control of synaptic plasticity. *Trends Neurosci* **21**, 273–278.

Perea G & Araque A (2009). GLIA modulates synaptic transmission. *Brain Res Rev* .

Perin-Dureau F, Rachline J, Neyton J & Paoletti P (2002). Mapping the binding site of the neuroprotectant ifenprodil on NMDA receptors. *J Neurosci* **22**, 5955–5965.

Peters S, Koh J & Choi DW (1987). Zinc selectively blocks the action of N-methyl-D-aspartate on cortical neurons. *Science* **236**, 589–593.

Piña-Crespo JC & Gibb AJ (2002). Subtypes of NMDA receptors in new-born rat hippocampal granule cells. *J Physiol* **541**, 41–64.

Popescu G & Auerbach A (2003). Modal gating of NMDA receptors and the shape of their synaptic response. *Nat Neurosci* **6**, 476–483.

Popescu G & Auerbach A (2004). The NMDA receptor gating machine: lessons from single channels. *Neuroscientist* **10**, 192–198.

Punnakkal P, Berberich S, Mishina M, Seeburg P & Köhr G (2006). Probing the number and function of triheteromeric NMDA receptors in synapses. Program No. 533.5. 2006 Neuroscience Meeting Planner. Atlanta, GA: Society for Neuroscience, 2006.

Pérez-Otaño I, Schulteis CT, Contractor A, Lipton SA, Trimmer JS, Sucher NJ & Heinemann SF (2001). Assembly with the NR1 subunit is required for surface expression of NR3A-containing NMDA receptors. *J Neurosci* **21**, 1228–1237.

Ramoa AS, Mower AF, Liao D & Jafri SI (2001). Suppression of cortical NMDA receptor function prevents development of orientation selectivity in the primary visual cortex. *J Neurosci* **21**, 4299–4309.

Roche KW, Standley S, McCallum J, Dune Ly C, Ehlers MD & Wenthold RJ (2001). Molecular determinants of NMDA receptor internalization. *Nat Neurosci* **4**, 794–802.

Rock DM & Macdonald RL (1992). The polyamine spermine has multiple actions on N-methyl-D-aspartate receptor single-channel currents in cultured cortical neurons. *Mol Pharmacol* **41**, 83–88.

Rock DM & Macdonald RL (1995). Polyamine regulation of N-methyl-D-aspartate receptor channels. *Annu Rev Pharmacol Toxicol* **35**, 463–482.

Rosenmund C, Stern-Bach Y & Stevens CF (1998). The tetrameric structure of a glutamate receptor channel. *Science* **280**, 1596–1599.

Rothman SM & Olney JW (1995). Excitotoxicity and the NMDA receptor–still lethal after eight years. *Trends Neurosci* **18**, 57–58.

Rumbaugh G & Vicini S (1999). Distinct synaptic and extrasynaptic NMDA receptors in developing cerebellar granule neurons. *J Neurosci* **19**, 10603–10.

Sakimura K, Kutsuwada T, Ito I, Manabe T, Takayama C, Kushiya E, Yagi T, Aizawa S, Inoue Y, Sugiyama H & et al. (1995). Reduced hippocampal LTP and spatial learning in mice lacking NMDA receptor epsilon 1 subunit. *Nature* **373**, 151–5.

Sakurada K, Masu M & Nakanishi S (1993). Alteration of Ca2+ permeability and sensitivity to Mg2+ and channel blockers by a single amino acid substitution in the N-methyl-D-aspartate receptor. *J Biol Chem* **268**, 410–415.

Salazar G, Craige B, Love R, Kalman D & Faundez V (2005). Vglut1 and ZnT3 co-targeting mechanisms regulate vesicular zinc stores in PC12 cells. *J Cell Sci* **118**, 1911–1921.

Sans N, Petralia RS, Wang YX, Blahos J, Hell JW & Wenthold RJ (2000). A developmental change in NMDA receptor-associated proteins at hippocampal synapses. *J Neurosci* **20**, 1260–71.

Sasaki YF, Rothe T, Premkumar LS, Das S, Cui J, Talantova MV, Wong HK, Gong X, Chan SF, Zhang D, Nakanishi N, Sucher NJ & Lipton SA (2002). Characterization and comparison of the NR3A subunit of the NMDA receptor in recombinant systems and primary cortical neurons. *J Neurophysiol* **87**, 2052–2063.

Sather W, Dieudonné S, MacDonald JF & Ascher P (1992). Activation and desensitization of N-methyl-D-aspartate receptors in nucleated outside-out patches from mouse neurones. *J Physiol* **450**, 643–672.

Sather W, Johnson JW, Henderson G & Ascher P (1990). Glycine-insensitive desensitization of NMDA responses in cultured mouse embryonic neurons. *Neuron* **4**, 725–731.

Schneggenburger R, Zhou Z, Konnerth A & Neher E (1993). Fractional contribution of calcium to the cation current through glutamate receptor channels. *Neuron* **11**, 133–143.

Scimemi A, Fine A, Kullmann DM & Rusakov DA (2004). NR2B-containing receptors mediate cross talk among hippocampal synapses. *J Neurosci* **24**, 4767–77.

Sheng M, Cummings J, Roldan LA, Jan YN & Jan LY (1994). Changing subunit composition of heteromeric NMDA receptors during development of rat cortex. *Nature* **368**, 144–7.

Smart TG, Hosie AM & Miller PS (2004). Zn2+ ions: modulators of excitatory and inhibitory synaptic activity. *Neuroscientist* **10**, 432–442.

Sobolevsky AI, Rosconi MP & Gouaux E (2009). X-ray structure, symmetry and mechanism of an AMPA-subtype glutamate receptor. *Nature* **462**, 745–756.

Soderling TR & Derkach VA (2000). Postsynaptic protein phosphorylation and LTP. *Trends Neurosci* **23**, 75–80.

Sommer B, Köhler M, Sprengel R & Seeburg PH (1991). RNA editing in brain controls a determinant of ion flow in glutamate-gated channels. *Cell* **67**, 11–19.

Sprengel R & Single FN (1999). Mice with genetically modified NMDA and AMPA receptors. *Ann N Y Acad Sci* **868**, 494–501.

Steinert JR, Postlethwaite M, Jordan MD, Chernova T, Robinson SW & Forsythe ID (2010). NMDAR-mediated EPSCs are maintained and accelerate in time course during maturation of mouse and rat auditory brainstem in vitro. *J Physiol* **588**, 447–463.

Stephenson FA, Cousins SL & Kenny AV (2008). Assembly and forward trafficking of NMDA receptors. *Mol Membr Biol* **25**, 311–320.

Stern-Bach Y, Bettler B, Hartley M, Sheppard PO, O'Hara PJ & Heinemann SF (1994). Agonist selectivity of glutamate receptors is specified by two domains structurally related to bacterial amino acid-binding proteins. *Neuron* **13**, 1345–1357.

Stocca G & Vicini S (1998). Increased contribution of NR2A subunit to synaptic NMDA receptors in developing rat cortical neurons. *J Physiol* **507**, 13–24.

Sucher NJ, Akbarian S, Chi CL, Leclerc CL, Awobuluyi M, Deitcher DL, Wu MK, Yuan JP, Jones EG & Lipton SA (1995). Developmental and regional expression pattern of a novel NMDA receptor-like subunit (NMDAR-L) in the rodent brain. *J Neurosci* **15**, 6509–6520.

Sugihara H, Moriyoshi K, Ishii T, Masu M & Nakanishi S (1992). Structures and properties of seven isoforms of the NMDA receptor generated by alternative splicing. *Biochem Biophys Res Commun* **185**, 826–832.

Sun L, Margolis FL, Shipley MT & Lidow MS (1998). Identification of a long variant of mRNA encoding the NR3 subunit of the NMDA receptor: its regional distribution and developmental expression in the rat brain. *FEBS Lett* **441**, 392–396.

Swanson GT, Feldmeyer D, Kaneda M & Cull-Candy SG (1996). Effect of RNA editing and subunit co-assembly single-channel properties of recombinant kainate receptors. *J Physiol* **492**, 129–142.

Thomas CG, Miller AJ & Westbrook GL (2006). Synaptic and extrasynaptic NMDA receptor NR2 subunits in cultured hippocampal neurons. *J Neurophysiol* **95**, 1727–34.

Tombaugh GC & Sapolsky RM (1993). Evolving concepts about the role of acidosis in ischemic neuropathology. *J Neurochem* **61**, 793–803.

Tong G, Takahashi H, Tu S, Shin Y, Talantova M, Zago W, Xia P, Nie Z, Goetz T, Zhang D, Lipton SA & Nakanishi N (2008). Modulation of NMDA receptor properties and synaptic transmission by the NR3A subunit in mouse hippocampal and cerebrocortical neurons. *J Neurophysiol* **99**, 122–132.

Tovar KR & Westbrook GL (1999). The incorporation of NMDA receptors with a distinct subunit composition at nascent hippocampal synapses in vitro. *J Neurosci* **19**, 4180–8.

Traynelis SF, Burgess MF, Zheng F, Lyuboslavsky P & Powers JL (1998). Control of voltage-independent zinc inhibition of NMDA receptors by the NR1 subunit. *J Neurosci* **18**, 6163–6175.

Traynelis SF & Cull-Candy SG (1990). Proton inhibition of N-methyl-D-aspartate receptors in cerebellar neurons. *Nature* **345**, 347–350.

Traynelis SF, Hartley M & Heinemann SF (1995). Control of proton sensitivity of the NMDA receptor by RNA splicing and polyamines. *Science* **268**, 873–876.

Tsai G & Coyle JT (2002). Glutamatergic mechanisms in schizophrenia. *Annu Rev Pharmacol Toxicol* **42**, 165–179.

Tzingounis AV & Nicoll RA (2004). Presynaptic NMDA receptors get into the act. *Nat Neurosci* **7**, 419–20.

Vicini S, Wang JF, Li JH, Zhu WJ, Wang YH, Luo JH, Wolfe BB & Grayson DR (1998). Functional and pharmacological differences between recombinant N-methyl-D-aspartate receptors. *J Neurophysiol* **79**, 555–66.

von Engelhardt J, Doganci B, Jensen V, Hvalby O, Gongrich C, Taylor A, Barkus C, Sanderson DJ, Rawlins JN, Seeburg PH, Bannerman DM & Monyer H (2008). Contribution of hippocampal and extra-hippocampal NR2B-containing NMDA receptors to performance on spatial learning tasks. *Neuron* **60**, 846–60.

von Engelhardt J, Coserea I, Pawlak V, Fuchs EC, Köhr G, Seeburg PH & Monyer H (2007). Excitotoxicity in vitro by NR2A- and NR2B-containing NMDA receptors. *Neuropharmacology* **53**, 10–17.

Vyklický L (1993). Calcium-mediated modulation of N-methyl-D-aspartate (NMDA) responses in cultured rat hippocampal neurones. *J Physiol* **470**, 575–600.

Wafford KA, Bain CJ, Bourdelles BL, Whiting PJ & Kemp JA (1993). Preferential co-assembly of recombinant NMDA receptors composed of three different subunits. *Neuroreport* **4**, 1347–1349.

Watanabe M, Inoue Y, Sakimura K & Mishina M (1993). Distinct distributions of five N-methyl-D-aspartate receptor channel subunit mRNAs in the forebrain. *J Comp Neurol* **338**, 377–90.

Weitlauf C, Honse Y, Auberson YP, Mishina M, Lovinger DM & Winder DG (2005). Activation of NR2A-containing NMDA receptors is not obligatory for NMDA receptor-dependent long-term potentiation. *J Neurosci* **25**, 8386–90.

Westbrook GL & Mayer ML (1987). Micromolar concentrations of Zn2+ antagonize NMDA and GABA responses of hippocampal neurons. *Nature* **328**, 640–643.

Whittington MA & Traub RD (2003). Interneuron diversity series: inhibitory interneurons and network oscillations in vitro. *Trends Neurosci* **26**, 676–682.

Williams K (1993). Ifenprodil discriminates subtypes of the N-methyl-D-aspartate receptor: selectivity and mechanisms at recombinant heteromeric receptors. *Mol Pharmacol* **44**, 851–9.

Williams K (1994). Mechanisms influencing stimulatory effects of spermine at recombinant N-methyl-D-aspartate receptors. *Mol Pharmacol* **46**, 161–168.

Williams K (1997). Interactions of polyamines with ion channels. *Biochem J* **325**, 289–297.

Wo ZG & Oswald RE (1995). Unraveling the modular design of glutamate-gated ion channels. *Trends Neurosci* **18**, 161–168.

Wollmuth LP, Kuner T & Sakmann B (1998a). Adjacent asparagines in the NR2-subunit of the NMDA receptor channel control the voltage-dependent block by extracellular Mg2+. *J Physiol* **506**, 13–32.

Wollmuth LP, Kuner T & Sakmann B (1998b). Intracellular Mg2+ interacts with structural determinants of the narrow constriction contributed by the NR1-subunit in the NMDA receptor channel. *J Physiol* **506**, 33–52.

Wollmuth LP, Kuner T, Seeburg PH & Sakmann B (1996). Differential contribution of the NR1- and NR2A-subunits to the selectivity filter of recombinant NMDA receptor channels. *J Physiol* **491**, 779–797.

Wollmuth LP & Sobolevsky AI (2004). Structure and gating of the glutamate receptor ion channel. *Trends Neurosci* **27**, 321–328.

Wolosker H, Blackshaw S & Snyder SH (1999). Serine racemase: a glial enzyme synthesizing D-serine to regulate glutamate-N-methyl-D-aspartate neurotransmission. *Proc Natl Acad Sci U S A* **96**, 13409–13414.

Wong HK, Liu XB, Matos MF, Chan SF, Pérez-Otaño I, Boysen M, Cui J, Nakanishi N, Trimmer JS, Jones EG, Lipton SA & Sucher NJ (2002). Temporal and regional expression of NMDA receptor subunit NR3A in the mammalian brain. *J Comp Neurol* **450**, 303–317.

Yamakura T, Mori H, Masaki H, Shimoji K & Mishina M (1993). Different sensitivities of NMDA receptor channel subtypes to non-competitive antagonists. *Neuroreport* **4**, 687–690.

Yamazaki M, Araki K, Shibata A & Mishina M (1992). Molecular cloning of a cDNA encoding a novel member of the mouse glutamate receptor channel family. *Biochem Biophys Res Commun* **183**, 886–892.

Yashiro K & Philpot BD (2008). Regulation of NMDA receptor subunit expression and its implications for LTD, LTP, and metaplasticity. *Neuropharmacology* **55**, 1081–1094.

Yuzaki M (2004). The delta2 glutamate receptor: a key molecule controlling synaptic plasticity and structure in Purkinje cells. *Cerebellum* **3**, 89–93.

Zhang L, Zheng X, Paupard MC, Wang AP, Santchi L, Friedman LK, Zukin RS & Bennett MV (1994). Spermine potentiation of recombinant N-methyl-D-aspartate receptors is affected by subunit composition. *Proc Natl Acad Sci U S A* **91**, 10883–10887.

Zhang W, Howe JR & Popescu GK (2008). Distinct gating modes determine the biphasic relaxation of NMDA receptor currents. *Nat Neurosci* **11**, 1373–1375.

Zheng F, Erreger K, Low CM, Banke T, Lee CJ, Conn PJ & Traynelis SF (2001). Allosteric interaction between the amino terminal domain and the ligand binding domain of NR2A. *Nat Neurosci* **4**, 894–901.

Zorumski CF, Yang J & Fischbach GD (1989). Calcium-dependent, slow desensitization distinguishes different types of glutamate receptors. *Cell Mol Neurobiol* **9**, 95–104.

Zuo J, Jager PLD, Takahashi KA, Jiang W, Linden DJ & Heintz N (1997). Neurodegeneration in Lurcher mice caused by mutation in delta2 glutamate receptor gene. *Nature* **388**, 769–773.

7 Abstracts

Rauner C and Köhr G (2008) Voltage dependence of NMDA receptor-mediated post-synaptic currents in the hippocampal CA1 area. Acta physiologica, 192, S.183.

Rauner C, Berberich S, Köhr G (2008) NR1/NR2A/NR2B receptors in hippocampal synapses identified by voltage-dependent deactivation in the absence of Mg^{2+}. Program No. 36.16. 2008 Neuroscience Meeting Planner. Washington, DC: Society for Neuroscience, 2008.

Rauner C and Köhr G (2009) Deciphering the composition of hippocampal synaptic NMDA receptors using transgenic mice and pharmacology. Kloster Schöntal: Interdisciplinary center for neurosciences (IZN) Retreat, 2009.

Cetin AH, Knobloch HS, Hoffmann L, Rauner C, Landeck N., Seeburg PH, Grinevich V (2009) Cell-type specific targeting of oxytocin and vasopressin neurons in live rodents by recombinant adeno-associated virus. Program No. 685.12. 2009 Neuroscience Meeting Planner. Chicago: Society for Neuroscience, 2009.

Knobloch HS, Hoffmann LC, Cetin AH, Rauner C, Schwarz MK, Seeburg PH, Grinevich V (2009) Virus based targeting of oxytocin and vasopressin neurons: A new tool for functional anatomy and physiology of hypothalamic neuropeptides. 19th Neuropharmacology Conference, Chicago.

8 Acknowledgements

I want to thank everyone who supported me during my PhD studies, especially:

PD Dr. Georg Köhr for introducing me into the experimental research in a new field as well as for scientific and technical advice at all times.

Prof. Dr. Peter H. Seeburg for excellent working conditions in the Department of Molecular Neurobiology of the MPI.

Prof. Dr. Gert Fricker as second referee at the Faculty of Biosciences.

Prof. Dr. Hannah Monyer for providing $NR2B^{\Delta Fb}$ mice.

Dr. M. Mishina (University of Tokyo) for providing the $NR2A^{-/-}$ mice line.

Dr. Simone Astori for continuous technical and scientific support as well as for his friendship.

The members of my working group, Dr. Sven Berberich, Dr. Mario Trevino, Dan Du, Marina Fendel, and all colleagues and friends from the MPI, especially of the Department of Molecular Neurobiology, for the nice working and social atmosphere.

Dr. Simone Schievink, Ann-Marie Michalski, Liliana Layer, and Kristin Bobsin for their friendship and support during my time at the MPI.

All the staffs of the animal facility for animal care and all technical assistants at the Department of Molecular Neurobiology for genotyping the mouse lines.

The MPI workshop for technical help, in particular Mr. Rödel and Mr. Hauswirth.

Harald, my and his family for continuous support.